PREDICTION OF SHEAR STRENGTH IN HIGHER STRENGTH CONCRETE BEAMS WITH MODERATE WEB REINFORCEMENT

By

Jamil Ahmad

(2006-NUST-MS Ph.D Str-02)

A Thesis submitted in partial fulfillment of
the requirements for the degree of
Master of Science

In

National Institute of Transportation

School of Civil and Environmental Engineering

National University of Sciences and Technology

Islamabad, Pakistan

(2010)

This is to certify that

thesis entitled

PREDICTION OF SHEAR STRENGTH IN HIGHER STRENGTH CONCRETE BEAMS WITH MODERATE WEB REINFORCEMENT

Submitted by

Jamil Ahmad

Has been accepted towards the partial fulfillment

of

the requirements

for

Master of Science in Civil Engineering

Brigadier (Retired) Dr. Khaliq-ur-Rashid Kayani

National Institute of Transportation

School of Civil and Environmental Engineering

National University of Sciences and Technology Islamabad

PREDICTION OF SHEAR STRENGTH

IN HIGHER STRENGTH CONCRETE BEAMS

WITH MODERATE WEB REINFORCEMENT

By

Jamil Ahmad

A Thesis

of

Master of Science

Submitted to the

National Institute of Transportation

School of Civil and Environmental Engineering

National University of Sciences and Technology

Islamabad

In partial fulfillment of the requirements

For the degree of

Master of Science in Civil Engineering

2010

DEDICATED

TO

MY PARENTS, WIFE, KIDS, TEACHERS

AND

WELL WISHERS

ACKNOWLEDGEMENT

All praises and thanks to Almighty Allah. I am grateful to Allah Almighty who gave me strength and patience to complete my Masters in Structural Engineering. I express my gratitude and heartfelt thanks to my thesis advisor, Brigadiar (Retired) Khaliq-Ur- Rashid Kayani for his untiring guidance, extra ordinary patience, kindness and encouragement in making this effort success.

I am thankful to National Highway Authority, Military College of Engineering concrete laboratory staff and Technical Trade Training Battalion without the financial and technical assistance of whom it would not have been possible to carry out most of the experimental work. My special thanks to the administration of National Institute of Transportation for their help in completion of this thesis.

Special thanks are due to my parents and family for their prayers and patience during my commitments to study and encouraging me to complete my MSc.

ABSTRACT

An experimental investigation of shear strength of high strength concrete beams with moderate web reinforcement was conducted. Tests on six beams were performed. All beams were designed in accordance with the provision of ACI 318-05. Concrete with compressive strength of 6000 to 10,000 psi was used in beam specimens. The quantity of shear reinforcement provided was greater than the minimum required by ACI 318-05. Specimens were provided shear reinforcement at 9 inch center to center. Actual shear strength of each specimen was compared with the shear strength predicted using the provisions of ACI 318-05.

Several mix designs with high cement content, low water cement ratio, high quality Kiriana Hills (Sargoda) aggregates and some admixtures i.e super plasticizer and silica fumes were properly mixed, consolidated and cured to achieve high strength concrete.

TABLE OF CONTENTS

LIST OF FIGURES

LIST OF TABLES

LIST OF ABBREVIATIONS/NOTATIONS

HSC	High strength concrete
NSC	Normal strength concrete
$f_c^{/}$	Compressive concrete strength
f_y	Yield strength of tension reinforcement
M	Moment
M_n	Nominal moment strength according to ACI code
V	Shear force
s	Stirrups Spacing
ρ	Reinforcement ratio (As/bd)
b	Beam width
d	Effective beam depth
h	Overall height of beam
Fig	Figure
V_c	Shear strength provided by concrete
V_s	Shear strength provided by steel
a	Shear span
V_n	Nominal shear strength
A_s	Longitudinal steel area
w/c	Water cement ratio
Dia	Diameter
mm	Millimeter
in	Inch
psi	Pounds per square inch
kn	Kilonewton

Chapter-1

INTRODUCTION

1.1 GENERAL

The development of concrete technology has been a slow evolutionary process. The concept of achieving higher strength concrete (HSC) by varying water-cement ratio and air entrainment was discovered in 1919 and 1938 respectively. The introduction of new admixtures i.e. super plasticizers and cementitious materials eg silica fume and fly ash have allowed the production of highly workable concrete with superior mechanical properties and durability. This new class of concrete has been named as high strength concrete.

In the middle of twentieth century, the concrete with a compressive strength of 50 MPa was considered high strength. In 1965, 72 MPa concrete was industrially produced for the first time in United States for making columns of Lake Point Tower building in Chicago, USA. With the commercial availability of concrete of compressive strength higher then 150 MPa, many questions have been raised regarding the design provisions stipulated in ACI Building Code Requirements for Structural Concrete (2005). For Shear Design, ACI code contains a number of empirical equations for different types of loadings and different types of members. Most of the design parameters and equations are derived from results of experimental research programs using concrete with compressive strength less then 40 Mps. Therefore it is reasonable to question applicability of all the design provisions in 2005 ACI Code for higher strength concrete members.

1.2 ADVANTAGES OF HSC

Excellent durability and stiffness have made HSC widely used in offshore structures, columns for tall buildings, long span bridges and other highway structures.

Economy and reduction in the size of structures is an important advantage offered by HSC. HSC is likely to have a somewhat higher initial cost per unit volume than normal strength concrete (NSC). However, its use is likely to be justified by saving in overall cost of the structure. Major advantages of HSC are: -

- Reduction in self-weight and superimposed dead load with the accompanying saving in construction time.
- Reduction in the member size, resulting in increase in retainable space.
- The enhanced workability.
- The enhanced durability and service life.
- The enhanced mechanical properties.
- Ease of placement and compaction without segregation.
- High toughness.
- Volume stability and control of deformations.
- Rapid use of form works and reduced construction cost.
- Longer spans and wider member spacing.

1.3 WORK ON HSC IN PAKISTAN

Limited work on HSC has been done in Pakistan and is restricted to power stations and few long span bridges. Faisal Mosque, Thermal Power Station Muzzafargarh Chimineys and long span bridges at Motorway are few of the projects where HSC ranging from 6000 to 8000 psi compressive strength had been used. No other significant work on production of HSC and testing of its shear strength has been carried out in Pakistan.

Modern trends in the field of construction impels structural engineers in Pakistan to look into this field and work on mechanics of HSC produced using local materials and technology.

1.4 SCOPE

The scope of this research is to:

- Produce concrete of appropriate strength.
- Provide experimental data to examine the existing empirical expression of ACI code predicting shear capacity of reinforced concrete beam with web reinforcement.
- Suggest measures/methods for better prediction of shear strength of high strength concrete beam.

Chapter-2

SHEAR CHARACTERISTICS OF CONCRETE BEAM

2.1 SHEAR IN BEAMS

A beam resists load primarily by means of internal moments M and shears V. In the design of a reinforced concrete member, flexure controls the appropriation of the section sizes and arrangement of reinforcement to provide the necessary moment resistance. Limits are placed on the amounts of flexural reinforcement which can be used, to ensure that if failure was ever to occur, it would develop gradually, giving warning before failure. The beam is then proportioned for shear. Since a shear failure is frequently sudden and brittle, therefore the design for shear must ensure that shear strength equals or exceeds the flexural strength at all points in the beam. The manner in which shear failures can occur varies widely with the dimensions, geometry, loading and properties of members, Figure 2.1 a and b (Appendix I).

2.2 SHEAR STRENGTH IN REINFORCED CONCRETE BEAMS WITHOUT WEB REINFORCEMENT

The four mechanisms of shear transfer are: shear stresses, Vcz in uncracked concrete; interface shear transfer, often called “aggregate interlock” or “crack friction”, the dowel action of the longitudinal reinforcing bars; and arch action. Opinions vary about the relative importance of each mechanism in the total shear resistance, resulting in different models for members without transverse reinforcement. The forces transferring shear across an inclined crack in a beam without stirrups are illustrated in Figure, 2.2 (Appendix I).

The shear stresses in uncracked concrete are not very important for slender members without axial compression because the depth of the compression zone is relatively small. On the other hand, at locations of maximum moment for lesser slender beams, much of the shear is resisted in the compression zones, particularly after significant yielding of the longitudinal reinforcement.

Shear transfer in the interface is primarily due to aggregates that protruded from the crack surface and provided resistance against slip. However, as cracks go through the aggregate in lightweight and high-strength concrete, it still have the ability to transfer shear. The term 'friction' is appropriately used for the phenomenon.

Dowel action is not very significant in members without transverse reinforcement as the maximum shear in a dowel is limited by the tensile strength of the concrete cover supporting the dowel. Nevertheless, it may be significant in members with large amounts of longitudinal reinforcement, particularly when the longitudinal reinforcement is distributed in more than one layer.

The relative importance of the arch action is directly related to the shear span-to-depth ratio, *a/d* i.e. the distance from the support to the load over the effective depth as shown in Figure 2.3 (Appendix I). Beams without stirrups, with an a/d ratio of less than 2.5, develop inclined cracks and, after a redistribution of internal forces, are able to carry an additional load due in part to arch action. Figure 2.4 (Appendix I) shows how the failure shear strength of a simply-supported reinforced concrete beam loaded with two-point loads changes as the shear span changes. For these series of beams, tested by Kani (1979), the ultimate shear strength was reduced by a factor of about 6 as the a/d ratio increased from 1 to 7. As the beams contained a large amount of longitudinal reinforcement, flexural failures at mid span did not become critical until a

shear span-to-depth ratio of about 7. This study focuses on members whose a/d ratio is over 2.5.

2.3 SHEAR STRENGTH IN REINFORCED CONCRETE BEAMS WITH WEB REINFORCEMENT.

Ideally, the purpose of web reinforcement is to ensure that shear failure does not occur and that the full flexural capacity can be achieved. Prior to inclined cracking, the strain in the stirrups is equal to the corresponding strain in the concrete and, therefore, the stress in the stirrups prior to inclined cracking is relatively small. Stirrups do not prevent inclined cracks from forming as they come into play only after cracks have formed.

Figure 2.5 (Appendix I) shows the forces in a beam with stirrups after the development of an inclined crack. Between flexural and inclined cracking, the external shear is resisted by, V_{cz} (Shear in compression zone), V_{ay} (Vertical component of the shear transferred by aggregates interlock) and V_d (Dowel action). Eventually, the stirrups crossing the crack yield, the inclined crack opens more rapidly. As the inclined crack widens, V_{ay} decreases, forcing V_d and V_{cz} to increase at an accelerated rate until either a splitting failure occurs, or the compression zone crushes due to combined shear and compression.

Each of the components of this process except V_s (Shear in stirrups) has a brittle load deflection response. As a result, it is difficult to quantify the contribution of V_{cz} , V_d , V_{ay} . In design these are lumped together as V_c (Shear in concrete), referred to as "the shear carried by the concrete". Thus the nominal shear strength, V_n is assumed to be

$$V_n = V_c + V_s$$

2.4 SHEAR STRENGTH IN HIGH-STRENGTH CONCRETE BEAMS

As far as shear strength is concerned, Duthinh et al. (1996) assess that high-strength concrete presents us four main challenges:

- Current code provisions for shear strength design rely on empirical rules whose database is largely below 40 MPa. New design rules would have to rely on either rational methods or on tests that cover a higher range of strengths. Much progress has been made in the last 25 years on rational methods for shear design and there is hope that the rules can be made more understandable from first principles of mechanics. It is likely that the rules can be made simple enough that they can be adopted by the design community in the not-too-distant future.
- Shear failure surfaces in high-strength concrete members are smoother than in normal-strength concrete members, with cracks propagating through coarse aggregate particles rather than around them. Since one of the shear transfer mechanisms across cracks is by aggregate interlock, this mechanism needs to be re-examined for high-strength concrete. Test results to date indicate that shear friction in HSC can be as low as 35% of that in NSC (Walraven, 1995).
- Minimum shear reinforcement must prevent sudden shear failure on the formation of first diagonal tension crack and, in addition, must adequately control the diagonal tension cracks at service load levels. To prevent a brittle failure, an adequate reserve of strength must be provided by the shear reinforcement after diagonal cracking of reinforced concrete beams. To control crack widths at service load levels, not only must a minimum amount of shear reinforcement be

provided, but the maximum stirrup spacing must also be limited. Due to the higher tensile strength of high-strength concrete, a higher cracking shear is expected and hence, would require a larger amount of minimum shear reinforcement (Yoon et al. 1996).

2.5 SHEAR STRENGTH IN HSC BEAMS WITH WEB REINFORCEMENT

Most research on shear strength in HSC beams has dealt with the minimum amount of web reinforcement. The number of experimental studies with higher amounts of web reinforcement is not as high as the number of studies of beams without web reinforcement.

In 1986, Elxanaty et al. (1986) tested three beams with web reinforcement. One of them was made of high-strength concrete. According to their tests, the use of HSC tends to prevent shear compression failure and to ensure a diagonal tension failure instead, thus increasing the effectiveness of shear reinforcement (Duthinh et al.. 1996)

In Spain, Aparicio, Calavera and Del Pozo (1997) tested seven full-scale prestressed and reinforced precast beams to study the crushing of the web. They also developed a strut and tie model with arch effect.

Fourteen HSC beams failing in shear were tested by Sarsam and Al-Musawi (1992), and Kong and Rangan (1998) tested 48 reinforced high-performance concrete beams with vertical shear reinforcement under combined bending moment and shear with a/d ratios ranging from 1.51 to 3.60. They also reported the results of a statistical analysis performed on 147 earlier test results. Both Sarsam et al. and Kong et al. concluded that a large coefficient of variation was obtained when HSC test beam results were compared with the predictions made by various code provisions.

The effect of concrete strength and minimum stirrups on shear strength of large members was studied by Angelakos in his doctoral theses in 1999, which was later

published by Angelakos, Bentz and Collins (2001). The experiments indicated that even members containing 16% more than the minimum amount of stirrups specified by the ACI Code will still have inadequate margins of safety.

2.6 CONCLUSIONS FROM DIFFERENT EXPERIMENTAL PROGRAMS

A number of experimental programs for the prediction of shear strength in the high strength concrete beams have been carried out. Important conclusions drawn by them are:

- The ACI Code shear design method for slender beams with stirrups is conservative (Andrew 1987).
- Stirrups carry very little shear prior to inclined cracking (Andrew 1987).
- As the amount of stirrups increased, the beams displayed improved ductility and failures were less sudden (Andrew 1987).
- After inclined cracking, the stirrups stress increases at much faster rate in beams with low amount of stirrups (Andrew 1987).
- The concrete shear strength contribution, V_c, in beams with stirrups, may be as much as 30% lower than predicted by present ACI code equation. Nilson's results were more favorable for high strength concrete beams with stirrups as compared to beams without stirrups (Nilson 1995).
- The number of inclined cracks increased with increasing amount of web reinforcement, indicating an enhanced redistribution of internal forces in beams.
- The crack surfaces were observed to be much smoother in the higher strength concrete beams probably reducing the contribution of aggregate interlock to the shear strength of such beams.

- Beams without stirrups failed suddenly. These beams had only a single diagonal crack on one end of the beam extending throughout the shear span.
- Both shear and diagonal tension failure occur after yielding of the longitudinal reinforcement (Nilson 1998).
- Low amount of longitudinal reinforcement causes few but wider cracks while comparatively heavily reinforced beams fail with large but narrow cracks (Swamy 1985).
- The truss model analysis indicates that an increase in f'_c would increase the strength of the concrete component of the truss (Johnson 1989).

2.7 SHEAR THEORIES

2.7.1 Truss Model

The behavior of beams failing in shear must be expressed in terms of a mechanical/ mathematical model before designers can make use of this knowledge in design. The best model for beams with web reinforcement is the truss model. In 1899 and 1902, respectively, Ritter and Morsch, independently, published paper proposing the truss analogy for the design of reinforced concrete beams for shear. These procedures provide an excellent conceptual model to show the forces that exist in a cracked concrete beam.

As shown in Figure 2.6 and 2.7 (Appendix I), a beam with inclined cracks develops compressive and tensile forces, C and T, in its top and bottom flanges, vertical tensions in the stirrups and inclined compressive forces in the concrete diagonals between the inclined cracks. An analogous truss replaces this highly indeterminate system of forces.

2.7.2 Beam Theory

By the traditional theory for homogenous, elastic, uncracked beams, we can calculate the shear stresses, υ, on elements of a beam section as:-

$$v = \frac{VQ}{Ib} \tag{2.1}$$

where

V = Shear force on the cross section

Q = First moment about the neutral axis of the cross section

I = Moment of inertia of the cross section

b = Width of the member where the stresses are being calculated.

It should be noted that equal shearing stresses exist on both the horizontal and vertical planes through an element (Figure 2.5-Appendix I). The horizontal shear stresses are important in the design of construction joints, web-to-flange joints, or regions adjacent to the holes in beams. For an un-cracked rectangular beam, Eq 2.1 gives the distribution of shear stresses (Figure 2.5-Appendix I).

Generally, Eq 2.1 can not be applied to reinforced concrete beams for the following reasons:

- Reinforced concrete is a combination of two distinct materials whose strength and stiffness differ significantly and is not a homogenous material.
- Concrete is subjected to creep and therefore is not elastic.
- Cross sections may be cracked or uncracked. Since the extent of cracking at a specified location along the length of the beam is

unpredictable, the actual cross sectional properties on which to base computations of moment of inertia and moment of area can not be determined.

- Because of cracking, which varies unpredictably, the effective cross section of reinforced concrete members varies along their length. In continuous structures, variations in cross section influence the magnitude of internal forces.

Due to above-mentioned reasons, a precise evaluation of shear stress intensity is not possible for a reinforced beam. The ACI 2005 has therefore adopted a simple procedure for establishing the order of magnitude of the average shear stress on a cross section. The shear stress is computed by dividing the shear force by b_w d, the effective area of concrete.

$$v = \frac{V}{b_w d} \tag{2.2}$$

Where v = Shear stress at a section

V = Shear force at section

b_w = Width of beam web

d = Distance between compression surface and centroid of tension steel

2.7.3 Modified Compression Field Theory

The research has shown that, in general, the angle of inclination of the concrete compression is not 45º. Equations based on variable angle truss provide a more realistic basis for shear design. In addition, tests of reinforced concrete panels subjected to pure shear improved the understanding of the stress-strain characteristics of diagonally cracked concrete. These stress-strain relationships made it possible to develop an analytical model called the modified compression field theory. This theory proved capable of predicting accurately the response of reinforced concrete. The modified compression field model attempts to capture the essential features of the crack pattern idealized as a series of parallel cracks occurring at angle θ to the longitudinal direction (Mitchell and Collins).

The shear stress that can be transmitted across the crack is function of the crack width (w), aggregate size (a), is given as:

$$v_{ci} = \frac{2.16\sqrt{f_c^{/}}}{0.3 + \left(\frac{24w}{a + 0.63}\right)} \tag{2.3}$$

2.8 PROPOSED EMPIRICAL EQUATIONS

2.8.1 Theodore Zsutty's Equation

Zsutty used regression analysis to evaluate the empirical constant. The final proposed equation is:

$$V_n = 60\left(f_c^{/}\rho\frac{d}{a}\right)^{1/3} + rf_y \tag{2.4}$$

This equation is applicable to concrete compressive strength mostly varying from 2000 to 6000 psi.

2.8.2 Andrew G. Mphonde and Gregory C. Frantz

Based on inclined cracking and ultimate shear capacity, they proposed following equations:

$$V_n = \left(1.51\sqrt{f_c^{/}} + 90\right) + rf_y \tag{2.5}$$

$$V_n = \left(1.51\sqrt{f_c^{/}} + 135\right) + rf_y \tag{2.6}$$

Andrew G.Mphonde and Gregory C.Frantz proposed that the ultimate shear capacity of the beam with stirrups is best predicted by:

$$V_n = \left(1.51\sqrt{f_c^{/}} + 90\right) + 1.6rf_y \tag{2.7}$$

This uses the concrete distribution as the inclined cracking capacity of beam without stirrups.

2.8.3 ACI Equation

2.8.3.1 I.M.Viest first suggested the present format of ACI equation. Viest simplified the principal stress equation and suggested that shear strength of reinforced concrete beams may be obtained by using the relationship as follows:

$$V_c = \left[A + B\frac{\rho}{\sqrt{f_c^{/}}}\left(\frac{Vd}{M}\right)\right] bd\sqrt{f_c^{/}}$$

where

V_c = Shear stress causing diagonal cracking at a particular location

b = Width of the member

d = Effective depth of tensile reinforcement

$f_c^{/}$ = Concrete strength

ρ = Tensile steel ratio

A = Dimensional constant

B = Dimensional constant

$\frac{Vd}{M}$ = Shear span

ACI and ASCE constituted committee 420 in 1962 to carry out a statistical study for an equation evaluating the shear strength of reinforced non pre-stressed concrete beams. On the basis of statistical analysis of 440 beams, the following values of A and B are obtained:

A = 1.9

B = 2500

By replacing the values of the dimensionless constants:

$$V_c = \left(1.9\sqrt{f_c'} + 2500\rho\frac{V_u}{M_u}d\right)bd \le 3.5\sqrt{f_c'}bd \qquad (2.8)$$

2.8.4 Present Design Practices

Most existing design codes assume the shear resistance of a beam to be provided by the sum of the resistance due to:

- The concrete which is considered to be equivalent to the load causing diagonal cracking in a beam without shear reinforcement, referred to as the concrete contribution.
- The shear reinforcement.

The concrete contribution is taken as being equal to the shear force at the commencement of diagonal cracking. The shear strength has been formulated by different researchers using experimental data and analysing the major variables

affecting the shear strength such as reinforcement ratio, concrete strength, effective depth and a/d ratio.

2.8.4.1 ACI 318-05

ACI 318-05 equation is based on the assumption that the useful shear strength of a beam without shear reinforcement is exhausted, when inclined cracking start. The ultimate shear strength of beam having shear reinforcement is calculated from the following equation:

$$v_c = \left(1.9\sqrt{f_c^{/}} + 2500\rho\frac{V_u}{M_u}d\right)\text{psi} \tag{2.9}$$

Chapter 3

EXPERIMENTAL PROGRAM

3.1 GENERAL

A brief on the materials used and experimental/testing procedures followed for the research program are summarized in the succeeding paragraphs.

3.2 ESTABLISHMENT OF VARIABLES AND CONSTANTS

The concrete constituents used in the course of this research, based on availability of time and literature review were divided in two categories, the variable and constant constituents. W/C ratio and percentage of silica fumes were selected. The following constituents were kept constant (Arshad 2006).

- Use of indigenous construction materials with silica fume.
- Dosages and type of High range water reducing agent.
- Size and grading of coarse aggregate.
- Grading of fine aggregate.
- Size of reinforcement.

3.3 MATERIALS

3.3.1 Cement

The Type I cement conforming to ASTM C 150 and C 595 was used. Results of the tests carried out to ascertain the properties of cement are presented in Table 3.1 (Appendix II). Variation in the chemical composition and physical properties of the cement affect concrete compressive strength more than variations in any other single material.

3.3.2 Fine Aggregate

The required range of fineness modulus was 2.70 to 3.20 (Arshad 2006). Sand from Lawrancepur and Margala pan crush was mixed together to bring the value of

fineness modulus to 2.88. Results of the tests conducted for verification of properties of sand are tabulated in Table 3.2 (Appendix II). The gradation of the fine aggregate is tabulated in Table 3.3 (Appendix II), and graphically shown in Figure 3.1 (Appendix II).

3.3.3 Coarse Aggregate

Samples from Margala, Kiriana, and Kala Chita range being the well known sites for better quality of aggregates were collected. The laboratory test results for the three aggregate sources are tabulated in Table 3.4 (Appendix II). Comparison of the test results indicate that crushed aggregate from Kiriana hills had best physical properties.

For this research the quantity of coarse aggregate in all mix designs was kept constant. Maximum size for the aggregate was kept as 1/2 inches. For gradation purpose only three sizes were considered i.e. 1/2 inch, 3/8 inch, 3/16 inch. The gradation and sieve analysis was determined in accordance with ASTM C 136-93 and is tabulated in Table 3.5 (Appendix II), and graphically illustrated in Figure 3.2 (Appendix II).

3.3.4 Silica Fume (SF)

For the purpose of this research, SF was selected as a Pozzolanic cementitious material. SF produces best high early strength and durable concrete as compared to other pozzolanic materials (ACI 2005). The SF inclusion in the concrete mix increases the water demand and there by reduces the workability. More recently, the availability of high range water reducing agent has opened up new possibilities for the use of SF as part of the cementing material in concrete to produce very high strength or very high level of durability or both (ACI 2005). The chemical composition of the SF is tabulated in Table 3.6 (Appendix II).

3.3.5 High Range Water Reducing Agent

The High Range Water Reducing Agent used in the research, is a modified "polycarboxlate" type agent. The dosage was kept constant throughout the research

work as 4 per cent by weight of cementitious materials. The technical data of polycarboxlate is tabulated in Table 3.7 (Appendix II).

3.3.6 Mixing Water

Potable water from Nowshera was used for entire experimental work while curing compound was used for curing.

3.4 WORKABILITY OF FRESH CONCRETE

The concept of low w/c ratio retards the characteristics of fresh concrete workability to its minimum. By use of High Range Water Reducing Agent the reduction in workability due to low w/c ratios is improved. Slump of 48 mm for 15-25% of SF was selected as constant in mix design (Arshad 2006) as tabulated in Table 3.8 (Appendix II).

3.5 WATER TO CEMENTITIOUS MATERIAL (W/C) RATIO

An important variable in achieving high strength concrete is the water to cement ratio. The relationship between w/c ratio and compressive strength which has been identified in normal strength concrete has been found to be valid for HSC as well. The use of chemical admixtures and other cementations materials have been proven generally essential for producing workable concrete with low w/c ratio. W/C ratio for HSC typically ranges from 0.20 to 0.5 (ACI 2005).

Mix was planned with low w/c ratio ranging from 0.22 to 0.23. Due to very low w/c ratio, workability problems were anticipated therefore polycarboxlate was used accordingly.

3.6 MIXING

The mixing of HSC ingredients is little different from normal strength concrete mixing. The concrete containing SF requires very careful and calculated mixing of ingredients. Over mixing of such concrete may produce adverse effect on strength

development of the concrete. While preparing concrete in the laboratory, the key is batching the SF at the appropriate time and mixing the concrete adequately. ASTM C 192, Standard Practice for Making and Curing Concrete Test Specimens in the Laboratory, recommends: "Mix the concrete, after all the ingredients are in the mixer, for 3 minutes, followed by a 3 minutes rest, followed by a 2 minutes final mixing". These recommended mixing times were found not enough to break down the agglomerations and to disperse the SF.

Therefore, the following procedure was adopted to mix the ingredients to attain the full dispersion of admixtures in the mix (Holland 2005):

- SF must always be added with the coarse aggregate and some of the water. Batching SF alone or first can result in head packing or balling in the mixer. Mix SF, coarse aggregates, and water for 0.5 minutes.
- Add the Portland cement and any other cementitious material if any. Mix for an additional 1.5 minutes.
- Add the fine aggregates and use the remaining water to wash in chemical admixtures added at the end of the batching sequence. Mix for 5 minutes, rest for 3 minutes, and mix for 5 minutes. If there are doubts that full dispersion and efficient mixing has not been accomplished, mix longer. However, SF concrete cannot be over mixed.

3.7 CASTING OF SPECIMEN

Casting of specimens was carried out as per ASTM C 192M – 02. Six beams were prepared along with 6 cylinders for each beam with detail in Table 3.9 to Table 3.14 (Appendix II).

3.7.1 Description of Specimens

The size and details of the specimens were decided in such a way that they should not fail in flexure. The section selected was 7 ½ x 10 inches with two # 8 bars and two # 4 bars bundled together at the bottom as shown in Figure 3.3 (Appendix II). The overall depth was kept as 10 inches and effective depth 'd' was kept as 8.25 inches. A total of six beams were cast and tested. The beams were designated as BS9-1, BS9-2, BS9-3, BS9-4, BS9-5 and BS9-6. The alphabet B indicates "Beam" and S means spacing between stirrups as 9 inches. The last digit means the serial number in the category.

3.7.2 Reinforcing Steel

All the longitudinal bars were # 8 and # 4 deformed bars. The web reinforcement used in the beam was # 3 bar hooked by 18 gauge steel wires. The stress-strain diagram of 1 inch bar is shown in Figure 3.4 (Appendix II). The Grade 60 steel was used for longitudinal bars and Grade 40 steel was used for web reinforcement. The tension test data is given in Table 3.15 (Appendix II).

3.7.3 Fabrication of Specimens

The specimens were cast in steel shuttering designed for the purpose. The shuttering was prepared in such a manner that it could be dismantled easily. The steel reinforcement cage was bound with 18 gauge steel wire .The cage was placed in the shuttering over the 1-inch spacers and tied up with the bars. The concrete for the beams was mixed in a rotary mixer hired from local market. The capacity of the mixer was 7 cubic feet. One batch was prepared for one beam and its associated test cylinders. In one batch, 2 bags of cement were used. The standard cylinders cast with beam were 5 to 6 in numbers for each batch. The beams and associated cylinders were covered with Anti sole E-10 and kept under similar environments. The shuttering was removed from

beams after 24 hours. During the process of removing shuttering few hairline cracks were observed. The cracks were observed for their depth and extent. It was established that the cracks had not penetrated into the core of the beam and were only surface cracks occurred by shrinkage due to excessive SF.

3.7.4 Specimen BS9-1 to BS9-3

Beams were cast on 2 Feb 2008. The web reinforcement was placed at 9 inches centre to centre spacing. Other details of the subject beams are tabulated in Table 3.17 (Appendix II). The detail of the materials used in each of these beams is tabulated in Table 3.18 (Appendix II).

3.7.5 Specimen BS9-4 to BS9-6

Beams were cast on 6 April 2008. The web reinforcement was placed at 9 inches centre to centre. Other details of the subject beams are tabulated in Table 3.19 (Appendix II). The detail of the materials used in each of these beams is tabulated in Table 3.20 (Appendix II).

3.8 INSTRUMENTATION

Electrical strain gauges were fixed on web and longitudinal reinforcement for recording the strain at different points in shear span as well as in mid span region. All the beams (BS9-1, BS9-2, BS9-3, BS9-4, BS9-5, BS9-6), had one strain gauge fixed at the center and the other in shear span on longitudinal reinforcement, three strain gauges in shear span on web reinforcement of the beams. The electrical strain gauges of EA-06-240LZ-120/E nomenclature were used to record the strain in the beams. These gauges had 120.0 + 0.3% grid resistance in ohms with gauge factor 2.080 ± 0.5 at 24 ^{0}C. These gauges are manufactured with self-temperature compensation characteristics to minimize thermal output. The EA series gauges are a general purpose family of constant alloy strain gauges widely used in experimental stress analysis. EA gauges are

constructed with a 0.001-inch (0.03-mm) tough, flexible polyamide film backing. Strain gauges were soldered and checked with the help of digital multimeter.

3.8.1 Test Set Up

The specimens were transported to Structure Laboratory of University of Engineering and Technology Lahore, where a 50 ton universal testing machine made by Schmadu Tokyo, Japan, is installed. The machine is hydraulically operated and is connected to the computerized data acquisition system as shown in Figure 3.5 (Appendix II). Fifty (50) tons jack was used for the loading of specimens through a steel girder and base plates to create two point load system. The beams were placed on the supports with the help of a gantry crane.

3.8.2 Testing Procedure

Beams were divided into two groups, each group consisting of three beams. The beams were planned to be tested with a/d 2.5. The load was applied after centering and aligning the specimens on the testing machine and making all necessary corrections for recording the load, strain and deflection. The computer automatically acquired the strain, load and deflection data. During the application of load, the cracks were observed and marked on the beams.

Chapter 4

EXPERIMENTAL RESULTS

4.1 CONCRETE STRENGTH

Six cylinders were cast from each batch of concrete during the casting of the specimens. Three cylinders for BS9-4, BS9-5 and BS9-6 were tested after 28 days respectively, and the remaining three cylinders were tested on the day of the testing of beams, Table 4.1 to 4.3 (Appendix III).

4.2 STRAIN MEASUREMENTS

The strain was measured by using two electrical strain gauges on longitudinal reinforcement and three on web reinforcement.

4.3 TEST BEHAVIOR OF SPECIMENS

4.3.1 Specimen BS9-1

The beam was loaded on 26 April 2008 with shear span of 21 inches (a/d = 2.54). The reading from strain gauges, load cell and deflections were recorded using data acquisition system. The initial flexural cracks developed at 140 KN load. Increased load widened the flexural cracks and additional cracks appeared between 160 KN to 300 KN loads. Inclined cracks appeared at a load of 181 KN. Beam failed at 380 KN. Load deflection data and plot are given in Table 4.4 and Figure 4.1 (Appendix III), respectively. Load vs strains plot are shown in Table 4.10 and Figure 4.7 a and b (Appendix III), respectively. The crack pattern of the beam is shown in the Figure 4.12 a and b (Appendix III).

4.3.2 Specimen BS9-2

The beam was loaded on 25 April 2008 with a shear span of 21 inches (a/d = 2.54). Initial flexural cracks appeared at a load of 120 KN. Increased load widened the flexural cracks and additional cracks appeared from 160 to 237 KN load. Beam failed at a load of 280 KN. Load deflection data and plots are shown in Table 4.5 and Figure 4.2 (Appendix III). Cracking pattern is shown in Figure 4.13 a and b (Appendix III).

4.3.3 Specimen BS9-3

The beam was loaded on 25 April 2008 with a shear span of 21 inches (a/d = 2.54). Initial flexural cracks appeared at a load of 96 KN. Inclined cracks appeared at load of 179 KN and the beam failed at 260 KN. The cracking pattern shown in Figure 4.14 a and b (Appendix III). The load deflection and load strain data are shown in Table 4.6 and 4.11 (Appendix III). The load-deflection and load-strain plots are shown in Figures 4.3 and 4.8 a, b, c, d and e (Appendix III), respectively.

4.3.4 Specimen BS9-4

The beam was loaded on 26 April 2008 with a shear span of 21 inches (a/d = 2.54). Flexural cracks appeared at 96 KN. Increased load widened the flexural cracks and additional cracks appeared at 120 KN load. First inclined crack appeared at 160 KN after which more flexural were observed and old cracks also propagated. Inclined cracks kept on appearing along with propagation of few flexural cracks. Beam failed at a load of 300 KN. The cracking pattern is shown in the Figure 4.15 a and b (Appendix III). The load deflection data and load strain data are shown in Table 4.7 and 4.12 (Appendix III). The load deflection and load strain plots are shown in Figures 4.4 and 4.9 a, b, c and d (Appendix III).

4.3.5 Specimen BS9-5

The beam was loaded on 26 April 2008 with a shear span of 21 inches (a/d = 2.54). Flexural cracks appeared at 110 KN load. Inclined cracks occurred at 212 KN load. Inclined cracks widened with increase in load and beam failed at 280 KN. The load-deflection and load-strain data are shown in Table 4.8 and 4.13 (Appendix III). The load-deflection and load-strain plots are shown in Figures 4.5 and 4.10 a, b, and c (Appendix III). The cracking pattern is shown in Figure 4.16 a and b (Appendix III).

4.3.6 Specimen BS9-6

The beam was loaded on 26 April 2008 with a shear span of 21 inches (a/d = 2.54). The initial flexural cracks appeared at 110 KN load. Inclined cracks occurred at 176 KN load. By further increasing the load, the beam failed at a load of 380 KN. The load-deflection and load-strain data are shown in Table 4.9 and 4.14 (Appendix III). The load-deflection and load-strain plots are shown in Figures 4.6 and 4.11 a, and b (Appendix III). The cracking pattern is shown in the Figure 4.17 a and b (Appendix III).

4.3.7 Behavior of the beams during the tests can be summarized as under:

- Small flexural cracks occurred between 96 KN and 180 KN loads for shear span to depth ratio of 2.5.
- Extension of existing cracks and appearance of new flexural cracks in the shear span spreading from the load application sections towards the support. The flexural cracks in the shear spans tend to become more inclined.

- Sudden appearance of a wide diagonal shear crack in one of the shear span. In some cases this crack coincided partially with the inclined part of the flexural cracks. The occurrence of the shear crack was accompanied by drop in the load, which was easy to detect on automatic printed data.
- The average crack angle was between 35° and 45°.
- All beams failed suddenly with large widening of and sliding in one of the inclined cracks.
- Most of the beams failed in shear, except one (BS9 - 5 which failed in shear compression.

Chapter 5

ANALYSIS AND INTERPRETATION OF TEST RESULTS

5.1 GENERAL

Test data was analyzed to understand shear behavior of higher strength concrete beams with moderate web reinforcement. Shear strength of a beam varies with $f_c^{/}$, a/d ratio and amount of longitudinal reinforcement. Available data from literature was also used to draw logical conclusions.

5.2 GENERAL BEHAVIOR OF BEAMS

Five beams (BS9-1, BS9-2, BS9-3, BS9- 4 and BS9- 6) failed in diagonal shear, where as BS9-5 beam failed in shear compression. Flexural cracks appeared at mid spans during the early stages of loading. These cracks started at the bottom of the beams where flexural stresses are maximum. They appeared at shear loads of 140 KN, 120 KN, 96 KN, 96 KN, 110 KN, and 110 KN in BS9-1, BS9-2, BS9-3, BS9-4, BS9-5, and BS9-6 respectively. As the load increased, the existing cracks widened and new cracks developed in almost the entire length of the beams. Initial vertical flexural cracks in the shear span became inclined as they propagated above the longitudinal reinforcement. The inclined cracks at the ends of the beam are due to combined shear and flexure. These are commonly known as inclined cracks, shear cracks, or diagonal tension cracks. The average crack angle on the shear span was observed between 38 and 43 degrees. The inclined cracks in a beam with short shear span followed almost the straight line between the rollers at the load and at support. Since shear span and longitudinal reinforcement were kept constant in this experimental programme. The inclination may be related to the variation in the compressive strength of concrete. In

case of all six beams, the failure was preceded by large deflections due to yielding of the tensile reinforcement and sudden explosive/blast noise.

5.3 MECHANICS OF SHEAR RESISTANCE IN CONCRETE

5.3.1 From studies of shear models it is concluded that shear strength of reinforced concrete beams depends on following factors:

- Shear Strength of concrete section.
- Longitudinal reinforcement.
- Shear reinforcement.

5.3.2 Concrete Contribution (V_c)

5.3.2.1. ACI Equation:

Members subjected to shear and flexure are governed by fol ACI 38-2005 relation for calculation of shear capacity

$$V_c = 2\sqrt{f_c^{'}}bd \qquad 5.1$$

where

V_c = Shear strength provided by concrete

b = Web width

d = Distance from longitudinal tension reinforcement

$f_c^{/}$ = Specified compressive strength of concrete.

ACI building code has adopted the designs equation in which $\sqrt{f_c^{/}}$ is the main variable controlling the shear strength of concrete. The simplified ACI equation witch predicts

the shear strength of reinforced concrete beams without web reinforcement is of the form $2\sqrt{f_c^{/}}$ Figure 5.1& 5.2 (Appendix IV), show plot of observed shear strength of beams with $f_c^{/}$.

5.3.2.2 Effect of a/d (Shear span to depth) ratio. It is observed that the use of $\sqrt{f_c^{'}}$ as a sole predictor of V_c may be inappropriate. The shear span-to-depth ratio, a/d, should be considered as an important variable since it takes into account the length of the beam and its depth. Equation 5.1 is based on standard test data on 6 inch x 18 inch, prisms loaded at third points with a fixed a/d ratio of 1. It is believed that a/d ratio plays an important role in shear behavior of concrete beams as demonstrated in the dissertation, "prediction of shear strength in higher strength concrete beams without web reinforcement "(Khursheed 2008). The relationship of concrete shear strength is obviously inverse with shear span-to-depth ratio and directly proportional to concrete strength and can be expressed as under:

$$V_c = \frac{2\sqrt{f_c^{'}}bd}{a/d} \qquad 5.2$$

5.3.3. Longitudinal Reinforcement

5.3.3.1. Traditional beliefs and studies state that shear strength of a concrete section is influenced by the amount of longitudinal steel in term of their dowel action. It also reduces the width of cracks which may add to the aggregate interlock loss across the diagonal plane formed by the shear cracks. Longitudinal reinforcement provides resistance to applied shear depending upon the stress in longitudinal steel.

5.3.4 Web Reinforcement

5.3.4.1 Web shear reinforcement V_w, from beams with web reinforcement is the shear force in stirrups over a horizontal plane of area 'b x s':

$$V_w = \frac{A_v f_s}{bs}$$

by using

$$f_s = \alpha f_y$$

where the value of α = Ranges between 0 and 1.

Therefore:

$$V_w = \frac{\alpha A_v f_y}{bs} \qquad 5.3$$

5.4 SHEAR STRENGTH

5.4.1 General

Shear failures in reinforced concrete members are sudden and catastrophic in nature and should be catered for in the design. Normally, reinforced concrete members are first dimensioned for flexure and then checked for shear. The effect of shear is to induce tensile stresses on inclined planes oriented at approximately 45° to the plane on which the shear stresses act. Failure occurs when these stresses, along with horizontal stresses due to bending, exceed the diagonal tensile strength of the material. The failures occur in an inclined plane due to the combined effect of shear and flexural stresses. However, it is difficult to determine the value of the diagonal tensile stress in a reinforced concrete beam because the distribution of shear and flexural stresses over a cross section is not very certain. Accordingly, shear strength prediction in reinforced

concrete members is an empirical solution based on the assumption that a shear failure at the critical section occurs on a vertical plane when the average shear stress at that section, V/bd exceeds the member shear strength.

5.4.2 Cracking shear strength

The cracking shear strength V_{cr}/bd is defined as the shear strength at the occurrence of the initial diagonal crack. Cracking starts with the development of a few fine vertical flexural cracks at mid span, followed by reduction of bond between reinforcing steel and surrounding concrete in the support region. The diagonal cracks develop at about 1 ½ d to 2 d from the face of support. The cracking shear strength has to be linked with the amount of longitudinal reinforcement and the relationship is directly proportional. The cracking shear strength can be evaluated as:

$$V_{cr} = V_c + V_d + V_w \qquad 5.4$$

where $V_{cr} - V_c = V_d + V_w$

V_{cr} = Cracking shear strength

V_d = Shear due to dowel action of longitudinal reinforcement at cracking

V_c = Concrete shear strength

V_w = Force in shear reinforcement

5.4.2.1 It is believed that no significant stresses are induced in shear reinforcement till the formation of inclined cracks. Therefore, it can be assumed that $V_w \cong 0$ since force in transverse reinforcement is almost negligible till formation of cracks.

Accordingly $V_{cr} = V_c + V_d$.

5.4.2.2 Figure 5.8 (Appendix IV), shows plot of shear attributed to dowel action, $V_{cr} - V_c$ against measure of shear in longitudinal reinforcement which is dependent upon a/d ratio (Khursheed 2008). Basing on regression analysis of the results, the trend line shows $V_d = 0.3155\frac{A_s f_y}{a/d} + 17.761$ (Figure 5.8). A safe and conservative estimate based on available data for dowel action component of shear resistance can be made using following equation, which incidentally concides with data of beams without shear reinforcement(Khursheed 2008) :

$$V_d = 0.125\frac{A_s f_y}{a/d}$$

5.4.3 Ultimate shear strength

The ultimate shear strength v_u/bd is defined as the shear strength when failure occurs. The ultimate/failure shear strength is determined by the ability of the concrete to stabilize the first diagonal crack and to postpone further propagation of the crack into the compression zone. The ultimate shear strength can be:

$$V_n = V_c + V_d^{/} + V_w^{/} \qquad 5.5$$

$$V_d^{/} = V_n - V_c - V_w^{/} \qquad 5.6$$

$V_d^{/}$ = Shear due to dowel action at ultimate load

V_n = Nominal shear strength or total shear strength (V_t) by multiplying the strength reduction factor

$V_w^{/}$ = Web shear strength at ultimate load

V_c = Concrete shear strength

It is almost certain that web reinforcement will yield or almost to yield at failure. Hence $V_w^{/} \approx A_v f_y$. The concrete contribution, as already discussed, is $V_c = \frac{2\sqrt{f_c^{/}}bd}{a/d}$ at ultimate. In order to evaluate the dowel force at ultimate $V_t - V_c - V_w$ is plotted against $\frac{A_s f_y}{a/d}$. The regression analysis as in Figure 5.6 (Appendix IV), gives equation $V_d^{/} = 0.6201\frac{A_s f_y}{a/d} - 19.56$ for the experimental results. A safe and conservative estimate based for dowel action component of shear resistance can be made using following:

$$V_d^{/} = 0.4\frac{A_s f_y}{a/d}$$

The nominal shear strength of a reinforced concrete beam with web reinforcement can be estimated as: $V_t = V_c + V_d^{/} + V_w^{/}$

where $V_c = \frac{2\sqrt{f_c^{'}}bd}{a/d}$

$$V_w^{/} = A_v f_{yw}$$

f_{yw} = Yield stress of web reinforcement

$$V_d^{/} = 0.4\frac{A_s f_y}{a/d}$$

5.5 SHEAR STRENGTH RELATIONSHIPS

5.5.1 Cracking shear strength

From the previous section, an expression for determination of cracking shear force can be proposed as:

$$V_{cr} = \frac{2\sqrt{f_c^{/}}bd + 0.125A_s f_y}{a/d} \qquad 5.7$$

5.5.2 Ultimate shear strength

Similarly, the ultimate shear force of a beam can be computed:

$$V_t = \frac{2\sqrt{f_c^{/}}bd + 0.4A_s f_y + A_v f_{yw}}{a/d} \qquad 5.8$$

5.6 CONCLUSIONS

- ACI 2005 is very conservative in prediction of shear capacity of high strength concrete beams.
- Shear span to depth ratio affects the shear strength of the concrete. More is the ratio, lesser is the strength.
- Shear strength of concrete is directly proportional to the amount of longitudinal as well as the transverse reinforcement present in the beam.
- Shear strength of concrete is directly proportion to its compressive strength.

5.7 RECOMMENDATIONS FOR FUTURE WORK

It is not easy to understand mechanism of shear resistance. Extensive studies are required to be carried out for understanding of shear in concrete, taking into account of previous studies. Following are the suggested studies:

a. Development of shear resistance relationship with cross section development.

b. Effect of a/d ratio on shear strength.

c. Effect of compressive strength $f_c^{/}$, on shear strength to include very high concrete strength.

APPENDIX I

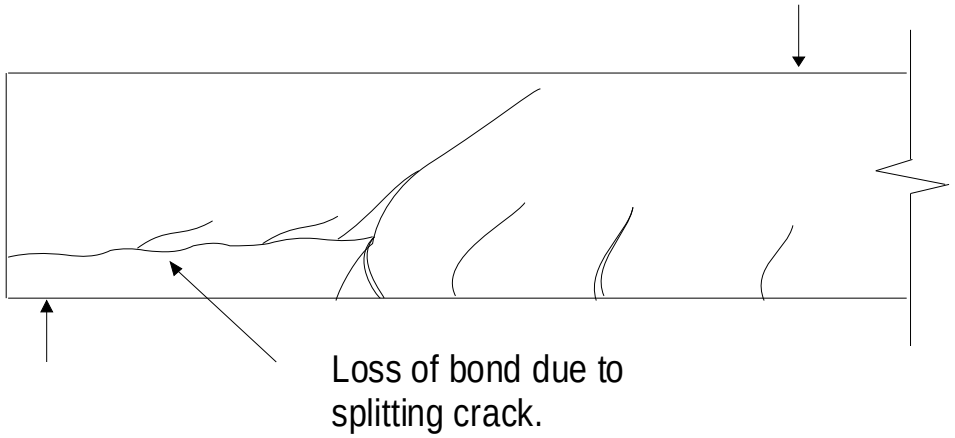

Fig 2.1a - Shear Tension Failure

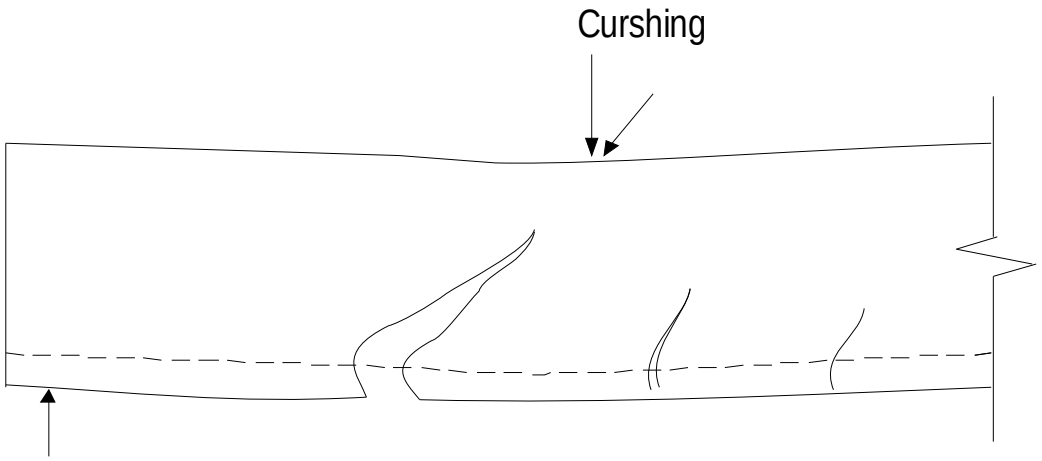

Fig 2.1b - Shear Compression Failure

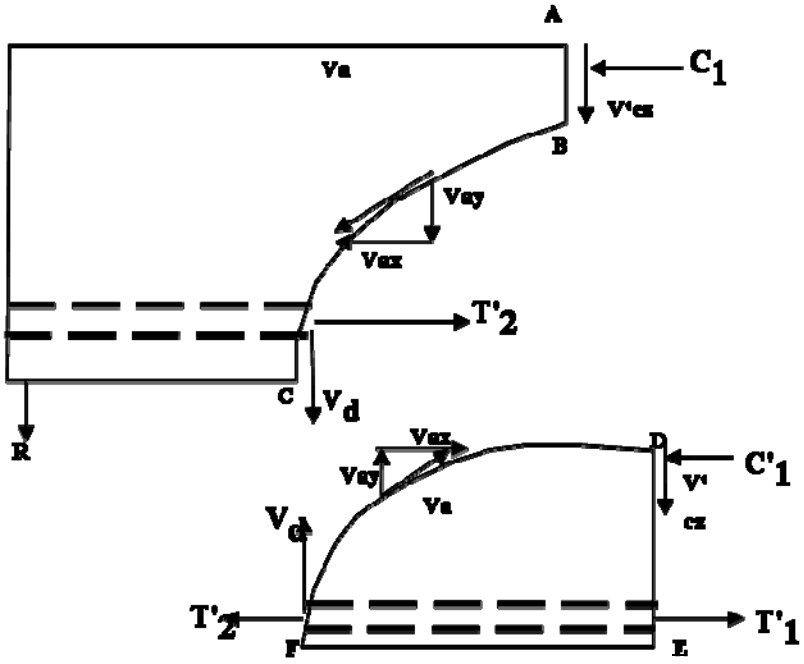

Fig 2.2 –Internal forces in a cracked beam without stirrups.

Fig 2.3 Shear Span

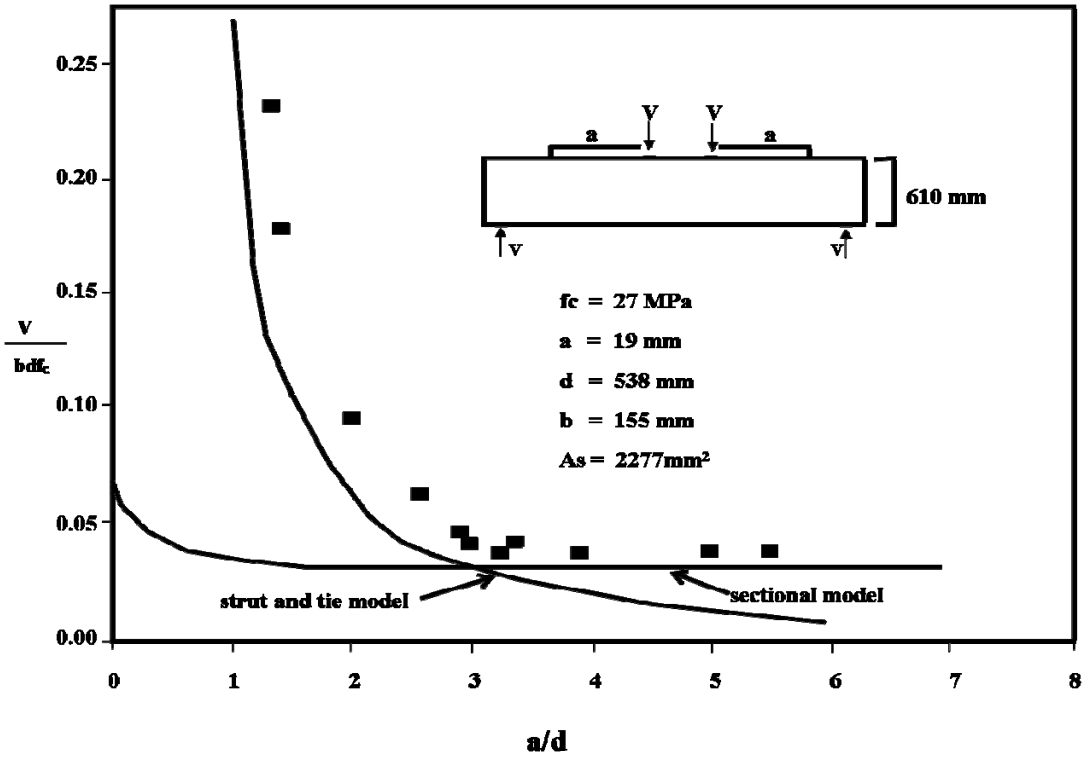

Fig 2.4 Predicted and observed strengths of a series of reinforced concrete beams tested by Kani (adapted from Collins and Mitchell 1997)

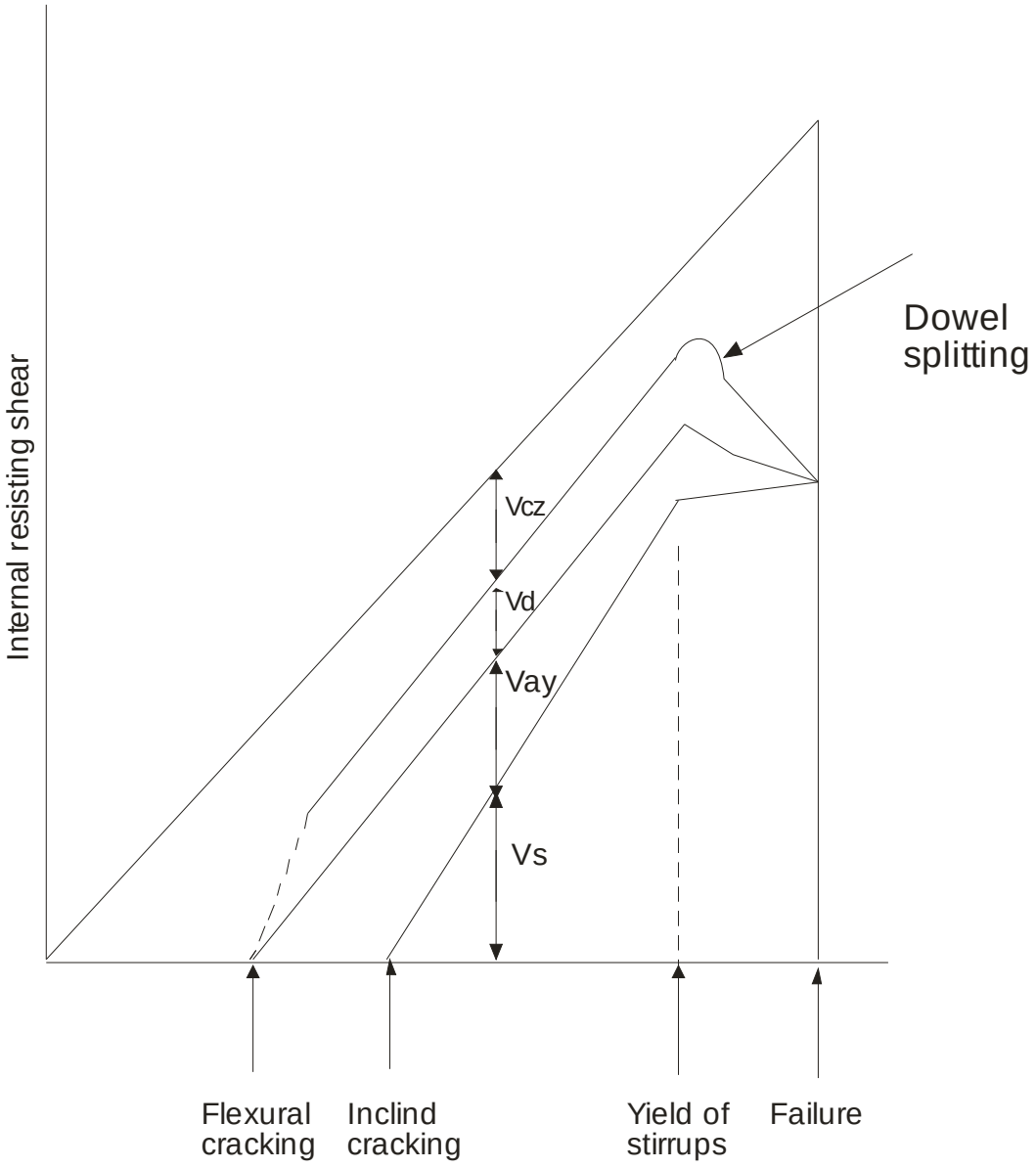

Fig 2.5 - Distribution of Internal Shear on a Beam

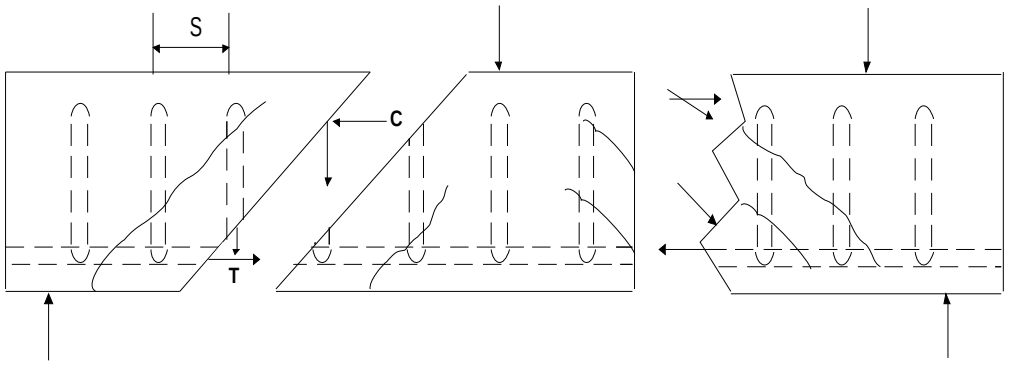

Fig 2.6 - Internal Forces in a Cracked Beam

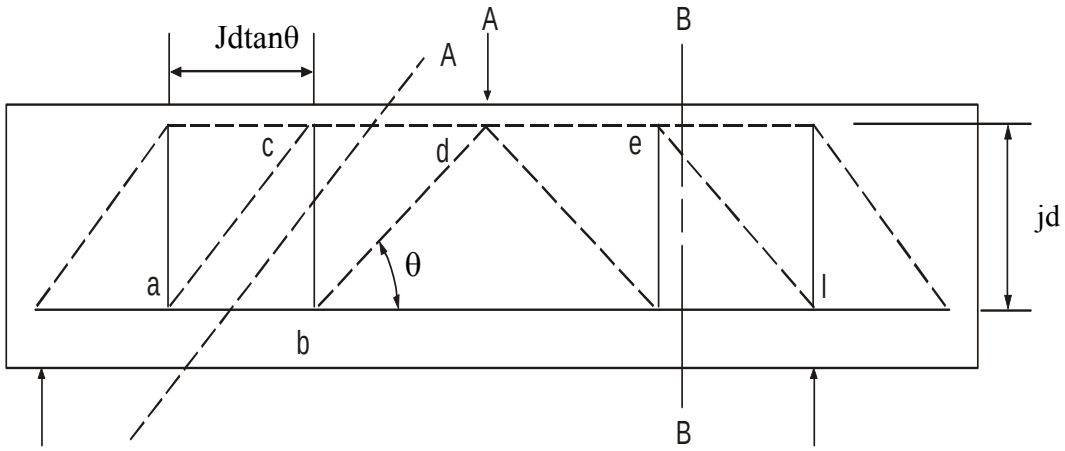

Fig 2.7 - Pin Jointed Truss

APPENDIX II

Table 3.1 - Properties of Cement

Properties of cement		
Tests	**Test results**	**Specifications**
Specific gravity	3.10	ASTM C 188
Initial setting time	150 minutes at 17^0C	ASTM C 191
Final setting time	390 minutes at 17^0C	ASTM C 191

Table 3.2 - Properties of Fine Aggregates

Properties of fine aggregates		
Tests	**Test results**	**Specifications**
Specific gravity	2.62	ASTM C 128
Absorption	0.01	ASTM C 128
FM	2.88	ASTM C 33

Table 3.3 - Gradation of Fine Aggregate

ASTM sieve No	**Weight retained (gm)**	**Percent retained**	**Cum percent retained**	**Percent passing**	
				Actual	**ASTM C 33 - 93**
#4	3	1	1	99	95-100
#8	46	9	10	90	80-100
#16	129	26	36	64	50-85
#30	146	29	65	35	25-60
#50	105	21	86	14	10-30
#100	43	9	95	5	2-10
#200	17	4			
Pan	7	1			

Table 3.4 - Comparisons of Aggregate Properties

Sample	Impact value (percent)	Crushing value (percent)	Abrasion value (percent)	Specific gravity
Margala	15.2	21.6	19.2	2.7
Kiriana	7.9	11.58	8.9	2.91
Kala Chita	16.2	22.5	19.2	2.81

Table 3.5 - Gradation of Coarse Aggregate

Sieve size (mm)	Percent retained	Cumulative percent retained	Percent passing	
			Actual	ASTM C 33 - 93
19	0	0	100	100
12.5	10	10	90	90-100
9.5	50	60	50	40-70
4.75	40	100	0	0-15

Table 3.6 - Chemical Compositions of SF

Chemical composition	Percentage
SiO_2	92
AI_2O_3	0.6
Fe_2O_3	1.0
CaO	0.4
MgO	1.5
K_2O	0.8
Na_2O	0.5

Table 3.7 - Technical Data of polycarboxlate

Attribute	**Aqueous solution of modified Polycarboxlate**
Appearance	Greenish liquid
Density	1.10 Kg / Liter
Ph-value	6.8

Table 3.8 - Workability of Mix

Percentage of silica fume	**Slump values (mm)**
	Using 4 per cent of High Range Water Reducing Agent
25	45

Table 3.9 - 28 days compressive strength of cylinders BS 9-1

Specimen	**Size of cylinders (mm)**	**Compressive strength 28 days (MPa)**
BS 9-1/1	152.4x304.8	46
BS 9-1/2	152.4x304.8	47
BS 9-1/3	152.4x304.8	47
BS 9-1/4	152.4x304.8	46
BS 9-1/5	152.4x304.8	46
BS 9-1/6	152.4x304.8	45
Average	-	46

Table 3.10 - 28 days compressive strength of cylinders BS 9-2

Specimen	**Size of cylinders (mm)**	**Compressive strength 28 days (MPa)**
BS 9-2/1	152.4x304.8	44
BS 9-2/2	152.4x304.8	46
BS 9-2/3	152.4x304.8	45
BS 9-2/4	152.4x304.8	46
BS 9-2/5	152.4x304.8	46
BS 9-2/6	152.4x304.8	4647
Average	-	46

Table 3.11 - 28 days compressive strength of cylinders BS 9-3

Specimen	**Size of cylinders (mm)**	**Compressive strength 28 days (MPa)**
BS 9-3/1	152.4x304.8	46
BS 9-3/2	152.4x304.8	47
BS 9-3/3	152.4x304.8	47.5
BS 9-3/4	152.4x304.8	46.5
BS 9-3/5	152.4x304.8	47
BS 9-3/6	152.4x304.8	46
Average	-	46.6

Table 3.12 - 28 days compressive strength of cylinders BS 9-4

Specimen	Size of cylinders (mm)	Compressive strength (MPa)	
		14 days	28 days
BS 9-4/1	152.4x304.8	59.5	68.7
BS 9-4/2	152.4x304.8	58	60.5
BS 9-4/3	152.4x304.8	57.5	60
Average	-	58.3	63

Table 3.13 - 28 days compressive strength of cylinders BS 9-5

Specimen	Size of cylinders (mm)	Compressive strength (MPa)	
		14 days	28 days
BS 9-5/1	152.4x304.8	56.7	67.2
BS 9-5/2	152.4x304.8	57.8	68.6
BS 9-5/3	152.4x304.8	57.7	68.2
Average	-	57.4	68

Table 3.14 - 28 days compressive strength of cylinders BS 9-6

Specimen	Size of cylinders (mm)	Compressive strength (MPa)	
		14 days	28 days
BS 9-6/1	152.4x304.8	60	69.8
BS 9-6/2	152.4x304.8	59.6	68.7
BS 9-6/3	152.4x304.8	60.2	69.9
Average	-	60	69.5

Table 3.15 - Stress Strain Curve Data (1" Dia Bar)

Load (tons)	Stress (psi)	Strain
0	0	0
1	3049.479	0
2	7280.392	0.000137
3	11511.3	0.000275
4	15742.22	0.000412
5	19973.13	0.000549
6	24204.04	0.000687
7	28434.95	0.000778
7.5	30550.41	0.000870
8.5	34781.32	0.000916
9	36896.78	0.001007
9.5	39012.24	0.001053
10	41127.69	0.001190
10.5	45358.6	0.001282
11	45358.6	0.001282
11.5	47474.06	0.001328
12	49589.52	0.001419
13	53820.43	0.001602
13.5	55935.89	0.001694
14	58051.34	0.001923
15	62282.25	0.023256
18	74947.99	0.046512
21	87667.73	0.093023
24	100360.5	0.162791
24.5	102475.9	0.209302
19.8	82590.63	0511628

Table 3.16 - Stress Strain Data (3/8" Dia Bar)

Load (tons)	Stress (psi)	Strain	Stress (psi)	Strain	Average Stress (psi)	Average Strain
	Specimen 1		Specimen 2			
0	0	0	0	0	0	0
1	20363.64	0.001361	20363.64	0.000875	20363.60636	0.001118
2	40727.27	0.003189	40727.27	0.0024	40727.27273	0.0027945
2.5	50909.09	0.037862	50909.09	-	50909.09091	0.037862
2.76	-	-	56203.64	0.03686	56203.64	0.03686
3	61090.91	0.7339	61090.91	-	61909.90909	0.7339
3.15	64145.45	0.086298	64145.45	-	64145.45455	0.086298
3.5	-	-	71272.64	0.005309	71272.64	0.005309
3.64	74123.64	-	74123.64	-	-	-
3.84	-	-	78196.4	-	-	-

Table 3.17 - Description of specimen BS 9-1 – BS 9-3

Description	BS 9-1 – BS 9-3
Design mix	1:0.7:1.7
Silica fume	25% by weight of cement
Viscocrete-1	4% by weight of cement
Mixing time	10 minutes
Cover on sides	1 inch
Cover from top/bottom	1 inch
No of cylinders cast	6
W/C ratio	0.22
Steel ratio	0.0646

Materials	Quantity (kgs)

Cement	279.6
Fine aggregate/pan	204.6/68.4
Coarse aggregate	642.6
Water	84.75
Silica fume 25%	96
Viscorete-1	14.19

Table 3.18 - Description of material BS 9-1 – BS 9-3

Table 3.19 - Description of specimen BS 9-4 – BS 9-6

Description	**BS 9-4 – BS 9-6**
Design mix	1:0.7:1.7
Silica fume	15% by weight of cement
Viscocrete-1	4% by weight of cement
Mixing time	10 minutes
Cover on sides	1 inch
Cover from top/bottom	1 inch
No of cylinders cast	6
W/C ratio	0.23
Steel ratio	0.0646

Table 3.20 - Description of material BS 9-4 – BS 9-6

Materials	**Quantity (kgs)**
Cement	319.26
Fine aggregate/pan	204.6/68.4
Coarse aggregate	642.6
Water	86.388
Silica fume 15%	18.783
Viscorete-1	14.19

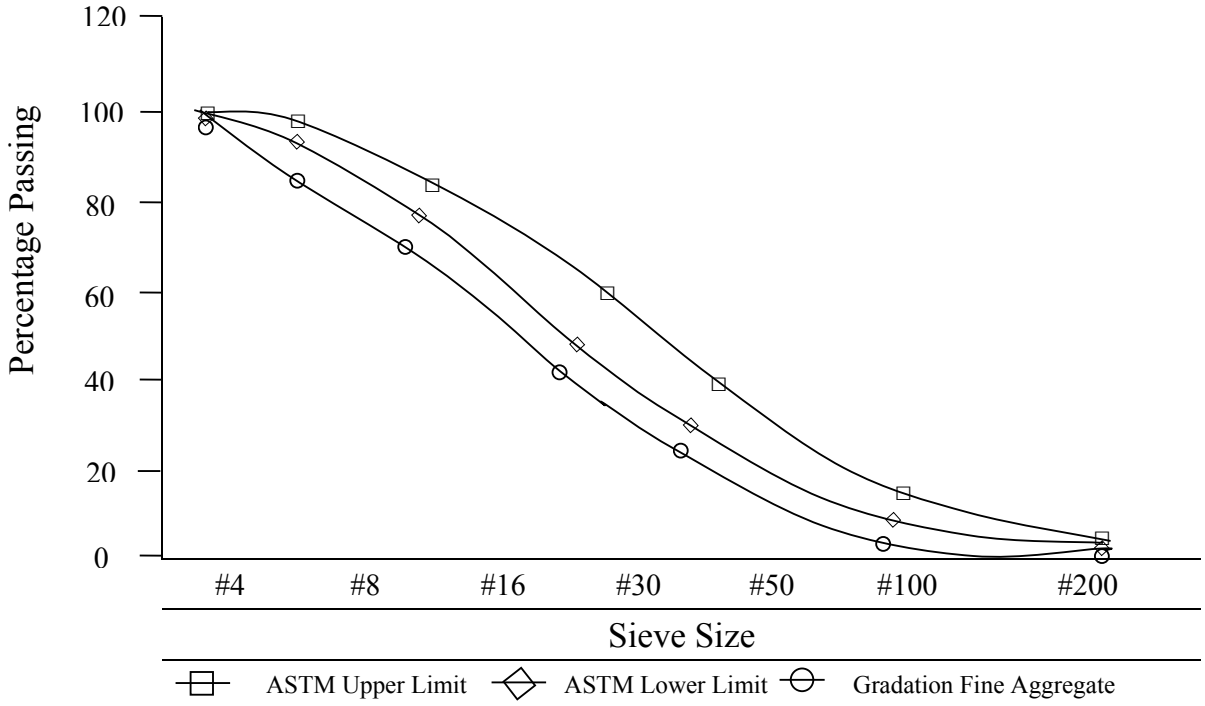

Fig 3.1 - Particle size distribution of fine aggregate

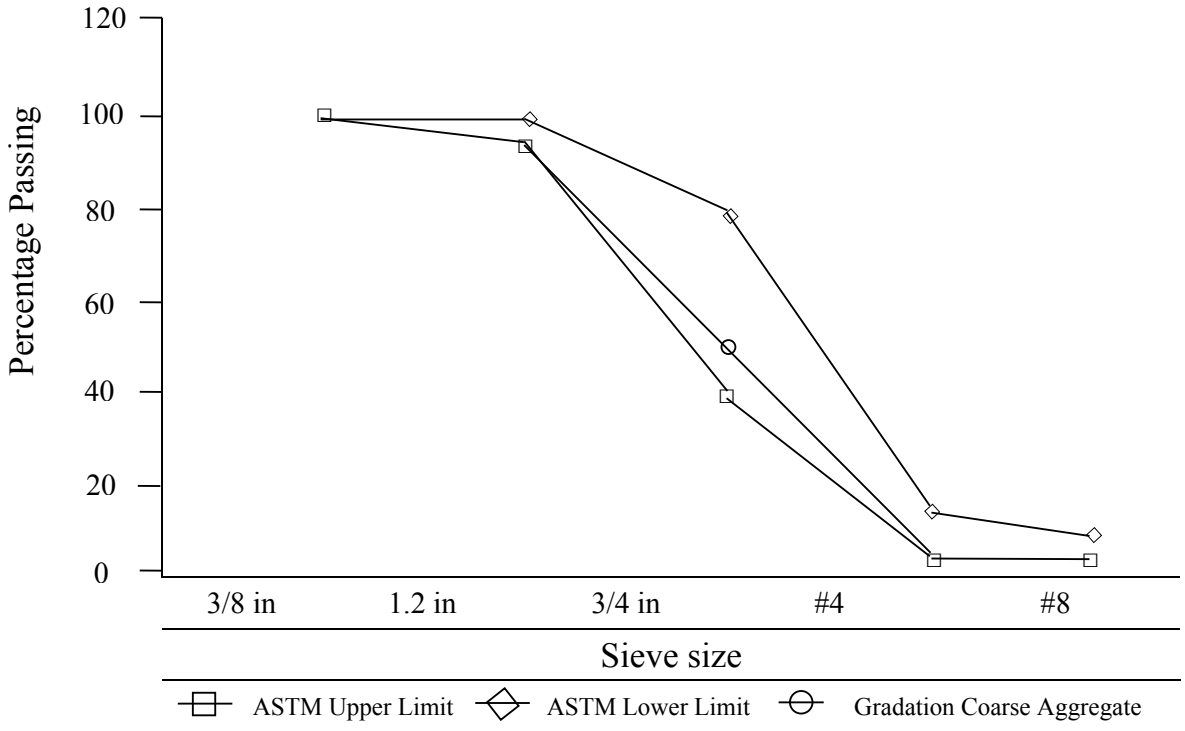

Fig 3.2 - Particle size distribution of coarse aggregate

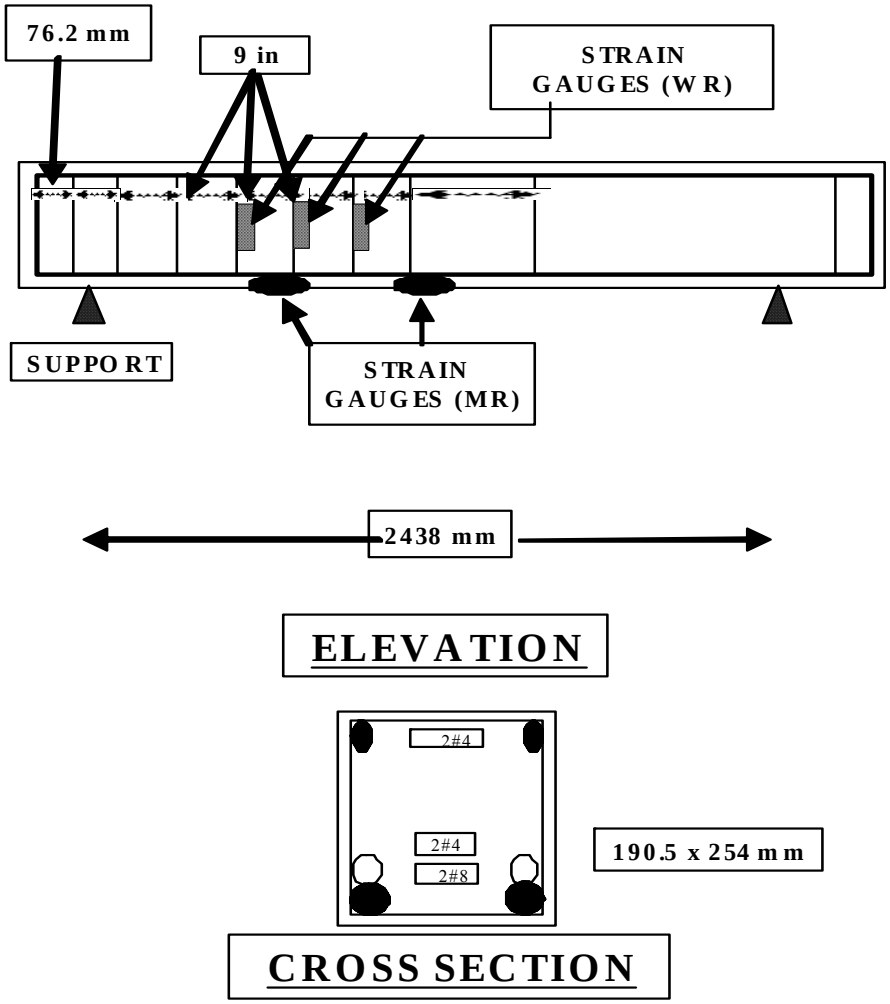

Fig 3.3 - Cross section of Beam

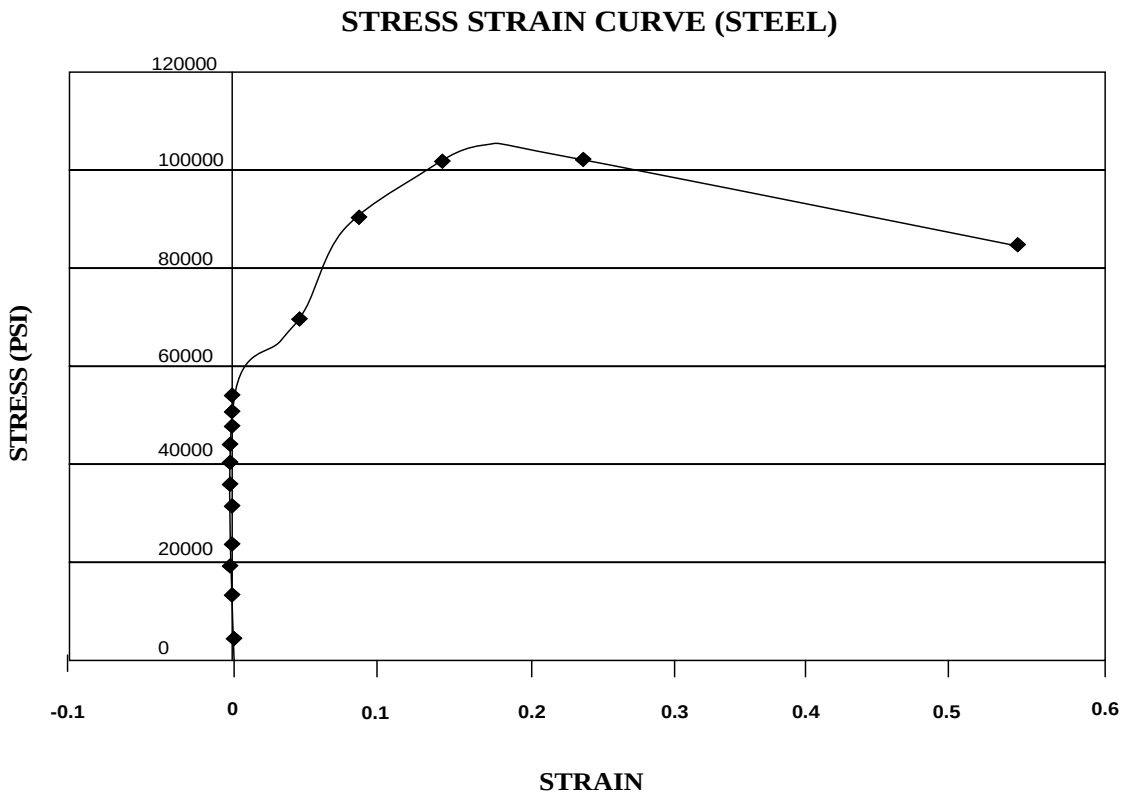

Fig 3.4 - Stress strain curve of 1" dia bar

Fig 3.5 - Test setup

APPENDIX III

Table 4.1 Compressive Strength on Day of Test BS 9-4

Specimen	Size of cylinders (mm)	Compressive strength (MPa)
BS 9-4/4	152.4x304.8	67.7
BS 9-4/5	"	67.3
BS 9-4/6	"	66.7
Average	-	67.3

Table 4.2 Compressive Strength on Day of Test BS 9-5

Specimen	Size of cylinders (mm)	Compressive strength (MPa)
BS 9-5/4	152.4x304.8	68.7
BS 9-5/5	"	69.1
BS 9-5/6	"	68.5
Average	-	68.7

Table 4.3 Compressive Strength on Day of Test BS 9-6

Specimen	Size of cylinders (mm)	Compressive strength (MPa)
BS 9-6/4	152.4x304.8	67.7
BS 9-6/5	“	69.3
BS 9-6/6	“	68.2
Average	-	68.4

Table 4.4 Load Deflection Data BS 9-1

LOAD (Kn)	**DEFLECTION (mm)**
0	0
20.03125	9.574
40.03125	10.736
60.09375	11.934
80	13.118
100	14.252
120	15.352
140	16.428
160	17.474
180	18.624
200.0625	19.742
220	21.416
240.0625	22.5
260	23.604
280	25.016
300	26.166
320	27.664
340	31.898
360	39.148
380	48.182
298.75	53.426
300.75	53.6

Table 4.5 Load Deflection Data BS 9-2

LOAD (Kn)	**DEFLECTION (mm)**
0	0
20	1.254
40	2.602
60	3.912
80	5.152
100	6.338
120	7.458
140	8.44
160	9.45
180.0625	10.372
200	12.952
220.0625	14.578
240	15.932
260	17.648
280	19.71
221.5625	24.254
217.6563	24.6

Table 4.6 Load Deflection Data BS 9-3

Load (kn)	**Deflection (mm)**
0	0
20	2.502
40	3.688
60	4.892
80	6.048
100	7.174
120	8.262
140	9.424
160	10.582
180	12.026
200	13.402
220.0313	14.526
240	15.68
260	17.23
220.0313	23.778
192.5625	28.636

Table 4.7 Load Deflection Data BS 9-4

Load (kn)	**Deflection (mm)**
0	0
20	6.866
40	8.316
60	9.848
80	11.222
100	12.562
120	13.752
140	14.876
160	15.958
180	17.016
200	18.078
240	21.088
260	22.414
280	23.94
300	25.774
277.656	27.52

Table 4.8 Load Deflection Data BS 9-5

Load (kn)	**Deflection (mm)**
0	0
20	5.418
40	6.736
60	8.02
80	9.214
100	10.378
120	11.472
140	12.56
160	13.834
180.125	15
200	16.318
220	17.568
240	19.186
260	24.51
280	36.26
279.5	40.528

Table 4.9 Load Deflection Data BS 9-6

Load (kn)	**Deflection (mm)**
0	0
40	1.76
60	3.052
80	4.108
100	5.018
120	5.854
140.0313	6.662
160	7.44
180	8.262
200	9.19
220	10.36
240	11.56
260	12.756
280	14.118
300	15.468
320	17.21
340	20.268
360	30.506
380	37.548

Table 4.10 Load Strain Data BS 9-1

Load (kn)	**Gauge 1 (mr)**	**Gauge 2 (mr)**
0	0	0
40.48966	200	174
60.85317	343	284
80.73207	469	416
100.4824	585	527
120.59866	699	641
140.78415	809	753
160.40591	918	862
180.53206	-174	976
200.4703	-191	1108
220.33931	-580	1248
240.39623	-471	1417
260.52238	-251	1616
280.39139	-182	1850
300.51754	-163	2157

Table 4.11 Load Strain Data BS 9-3

Load (kn)	Gauge 1 (mr)	Gauge 2 (mr)	Gauge 1 (wr)	Gauge 2 (wr)	Gauge 3 (wr)
0	0	0	0	0	0
20.05692	61	66	12	0	2
40.60834	149	193	32	11	20
60.54658	220	355	55	24	38
80.48482	286	547	81	34	56
100.90767	349	743	106	45	73
120.96459	405	948	128	56	87
140.0424	441	1115	144	66	116
160.09932	480	1288	161	69	147
180.22547	515	1474	179	84	273
200.77689	538	1703	197	91	368
220.89315	560	1883	212	98	551
240.08964	573	2003	227	102	704
260.15645	584	2133	243	105	875
280.63864	592	2317	258	109	1031
300.57688	595	2505	273	105	1318
320.88105	170	2790	303	95	3158
340.07754	158	3445	309	104	
235.50936	140	3149	287	88	
217.45486	131	2894	271	81	

Table 4.12 Load Strain Data BS 9-4

Load (kn)	Gauge 1 (mr)	Gauge 2 (mr)	Gauge 3 (wr)	Gauge 4 (wr)
0	0	0	0	0
20.79867	0	96	16	8
40.91493	0	222	29	16
60.54658	0	345	42	26
80.04966	-2	470	54	34
100.8483	1	556	63	40
120.0448	0	670	68	43
140.7842	0	794	81	45
160.0993	1	910	92	47
180.8387	0	1033	103	50
200.2231	0	1151	114	52
240.5248	0	1391	137	59
260.1565	-3	1508	145	61
300.8241	-4	1755	161	72
276.831	-51	6087	165	112
290.1825	-52	6135	167	113
300.0824	-50	6170	168	115
282.0529	-53	6104	166	113

Table 4.13 Load Strain Data BS 9-5

Load (kn)	Gauge1 (mr)	Gauge 2 (mr)	Gauge 3 (wr)
0	0	0	0
20.24483	-1164	71	18
40.11384	-1043	182	53
60.66526	-867	338	87
80.42548	630	84	
100.6604	838	109	
120.0448	1001	135	
140.2303	1161	166	
160.2279	1310	199	
180.0376	1459	235	
200.8362	1641		
220.5272	1794		
240.3369	1958		
260.1565	2114		
280.6485	3010		
279.7189	3011		
256.0917	2062		
216.3438	1762		

Table 4.14 Load Strain Data BS 9-6

Load (kn)	**Gauge 1 (mr)**	**Gauge 2 (mr)**
0	0	0
20.91735	139	150
40.91493	200	-173
60.23999	272	-403
80.85075	328	-757
100.17581	483	-2267
120.23273	594	-2179
140.47756	705	-2099
160.59382	812	-2025
180.34415	926	-1959
200.71755	1028	-1882
220.71513	1153	-1748
240.58414	1266	-1770
260.88831	1387	-1698
280.82655	1521	-1639
300.32963	1667	-1544

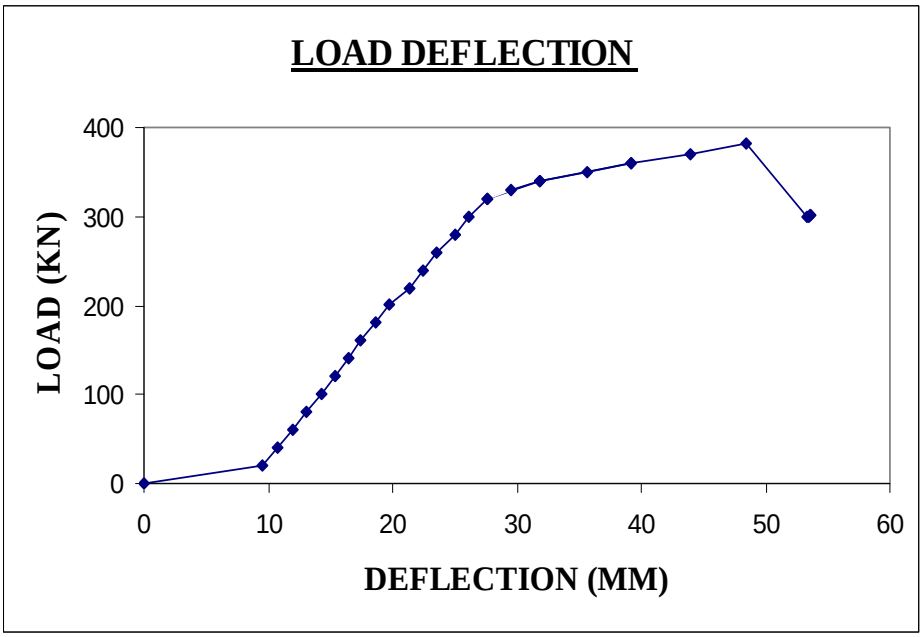

Fig 4.1 Load deflection behavior BS 9-1

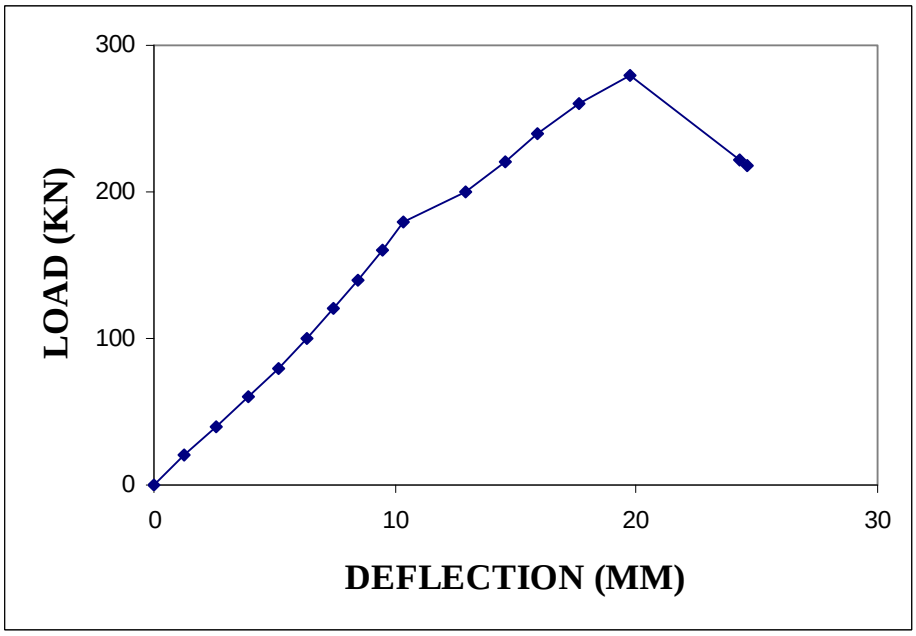

Fig 4.2 Load deflection behavior BS 9-2

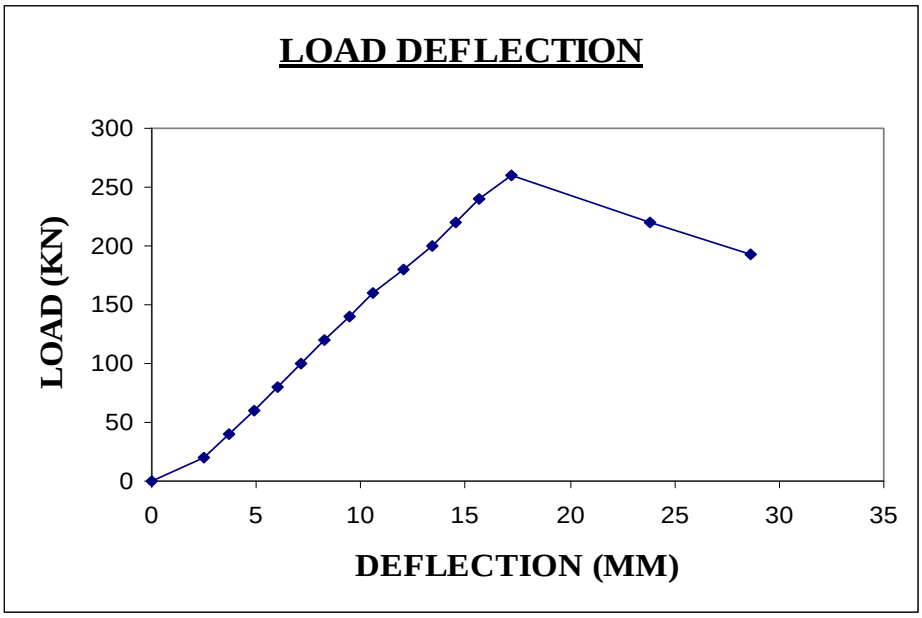

Fig 4.3 Load deflection behavior BS 9-3

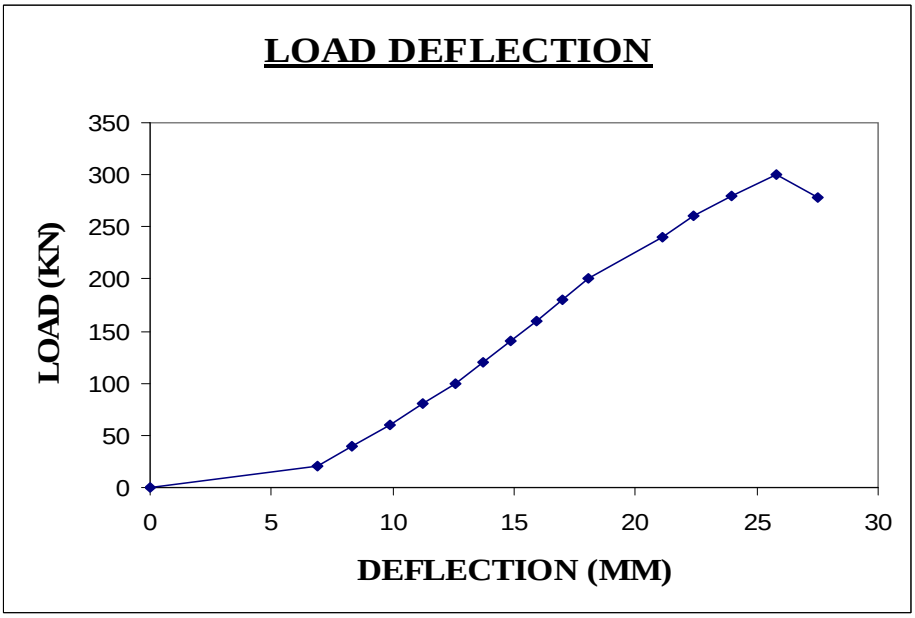

Fig 4.4 Load deflection behavior BS 9-4

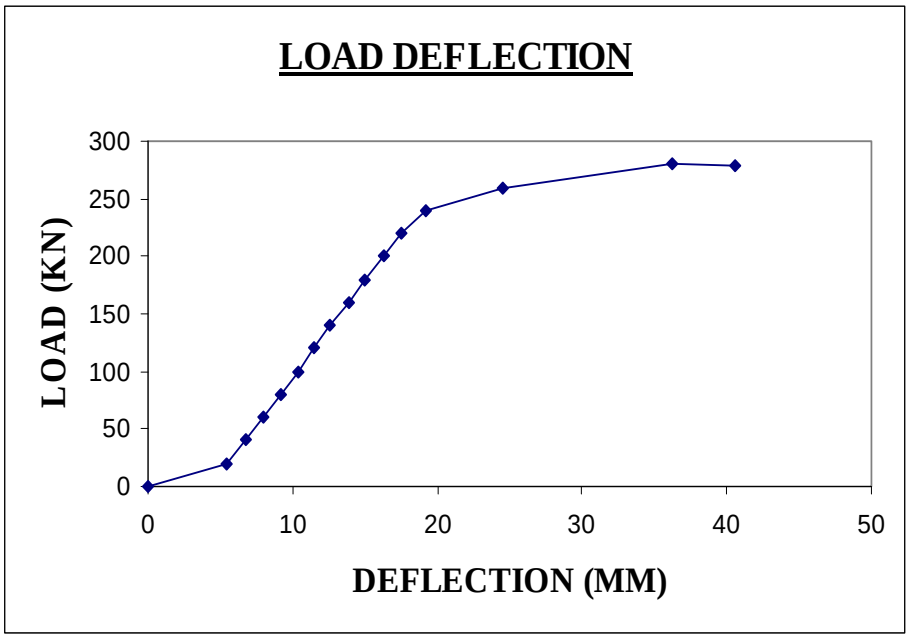

Fig 4.5 Load deflection behavior BS 9-5

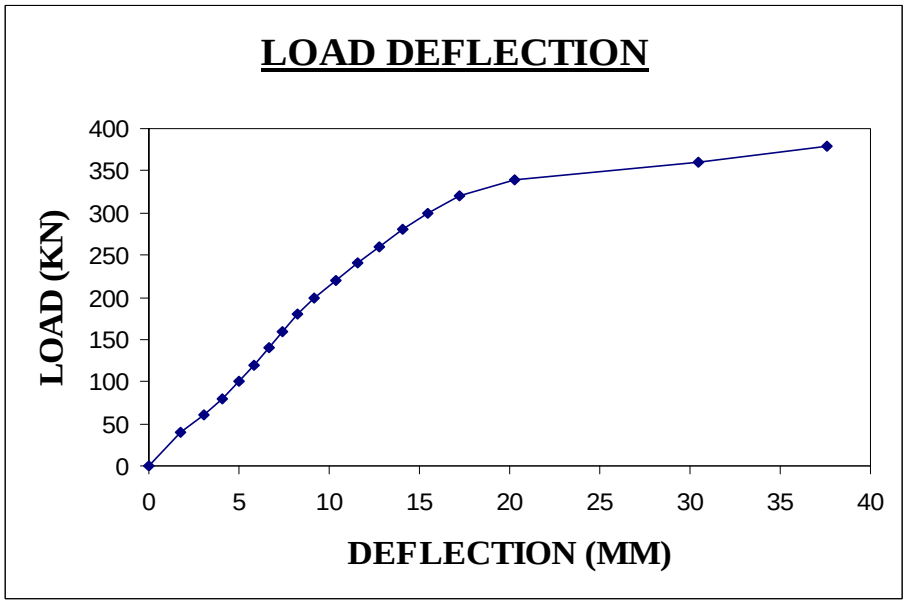

Fig 4.6 Load deflection behavior BS 9-6

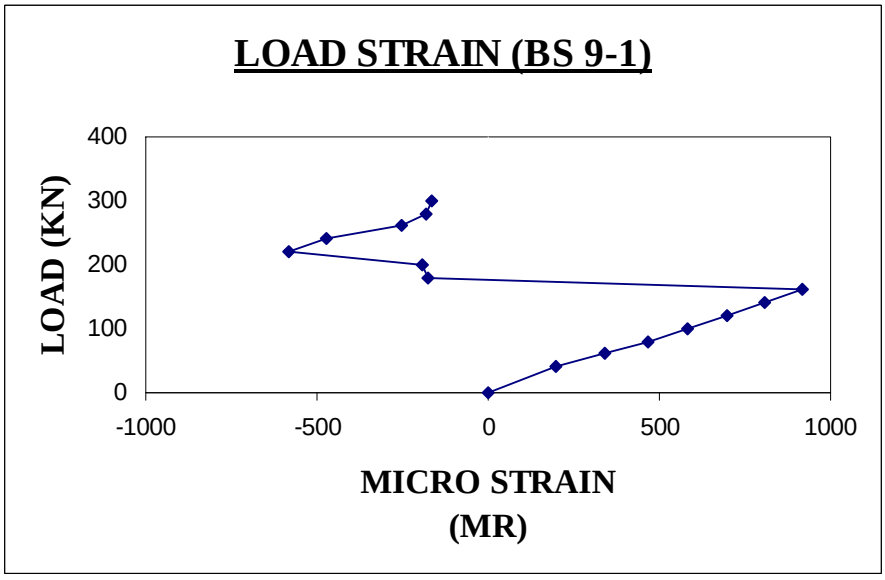

Fig 4.7 (a) Load strain behavior BS 9-1

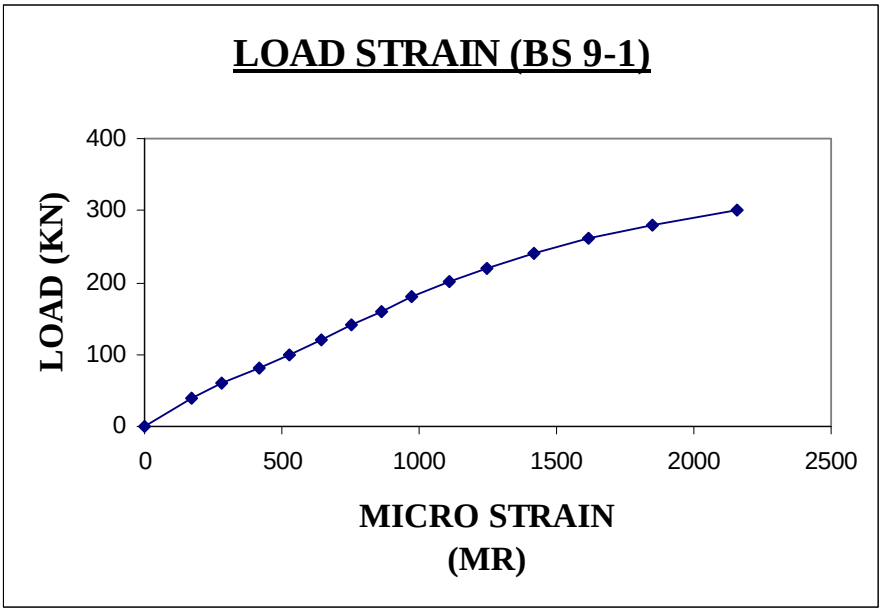

Fig 4.7 (b) Load strain behavior BS 9-1

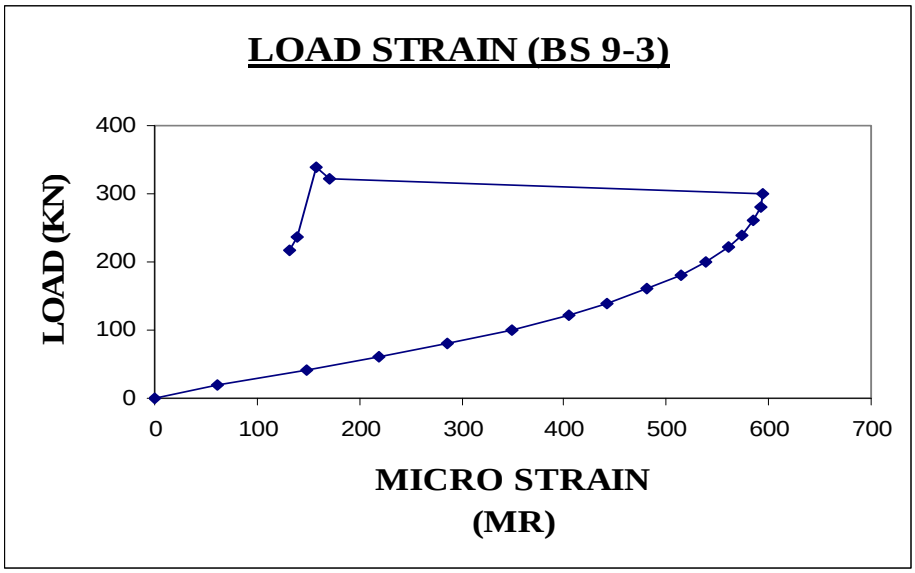

Fig 4.8 (a) Load strain behavior BS 9-3

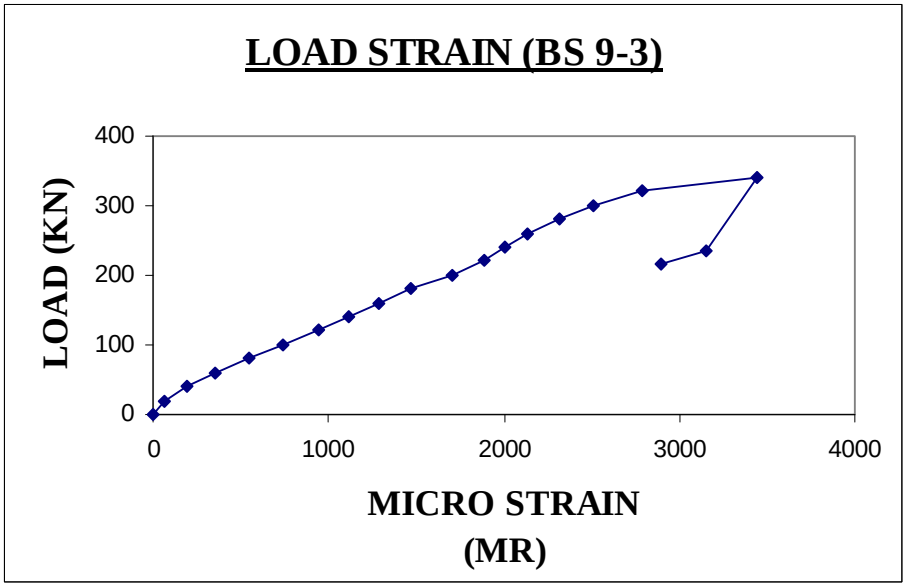

Fig 4.8 (b) Load strain behavior BS 9-3

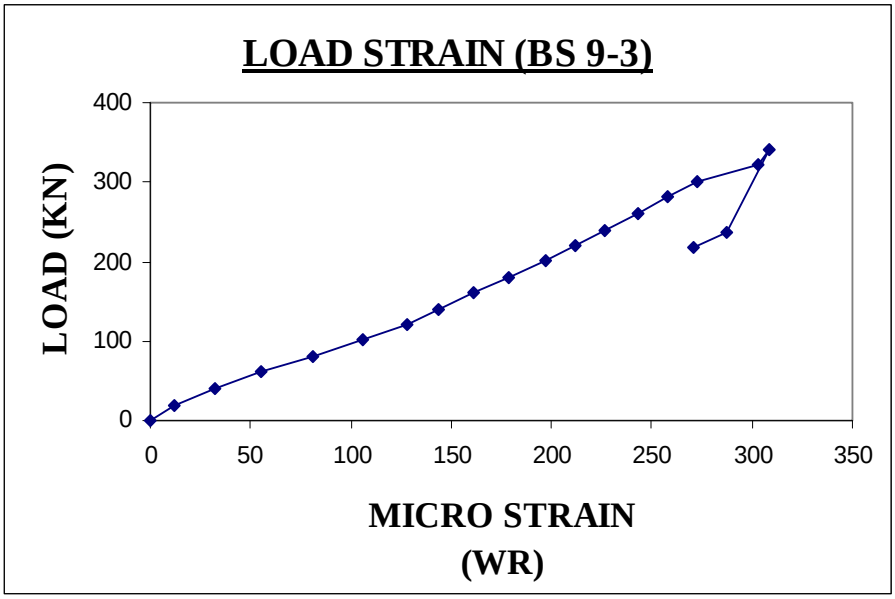

Fig 4.8 (c) Load strain behavior BS 9-3

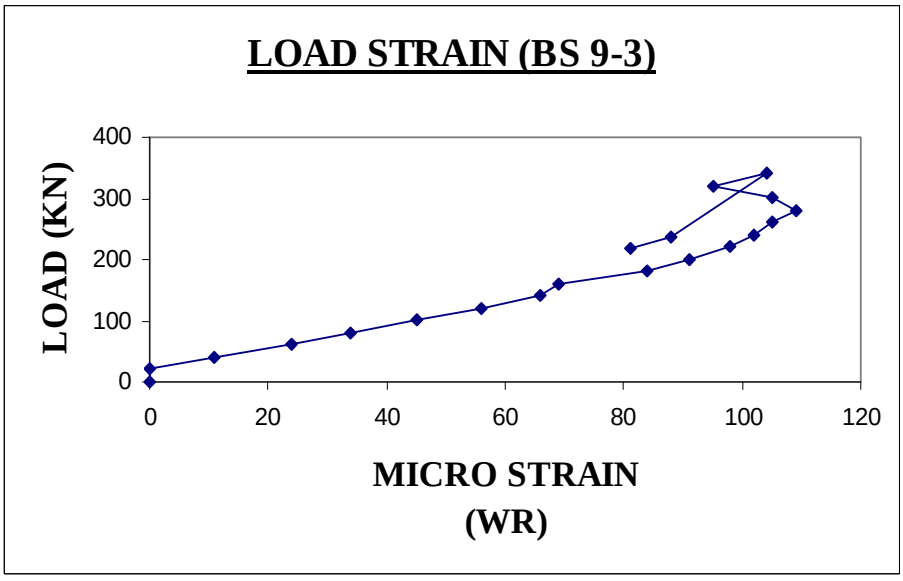

Fig 4.8 (d) Load strain behavior BS 9-3

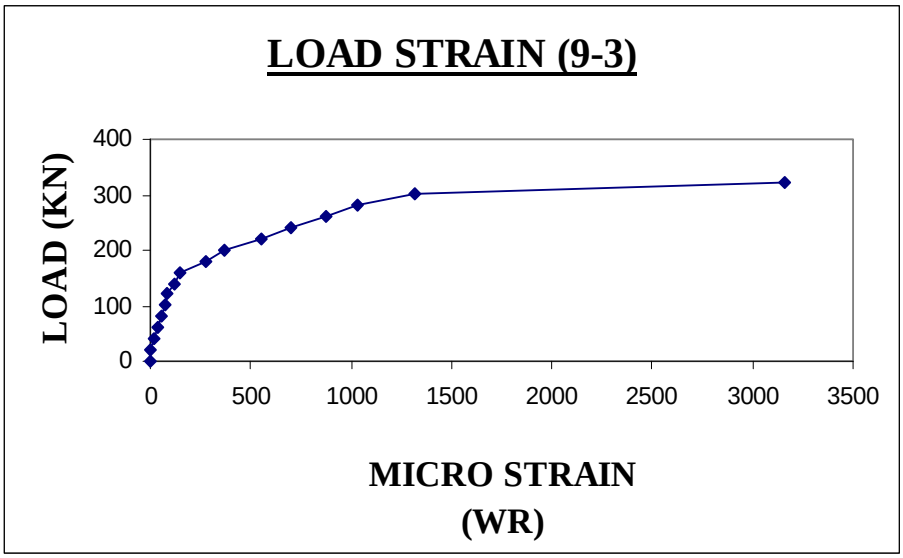

Fig 4.8 (e) Load strain behavior BS 9-3

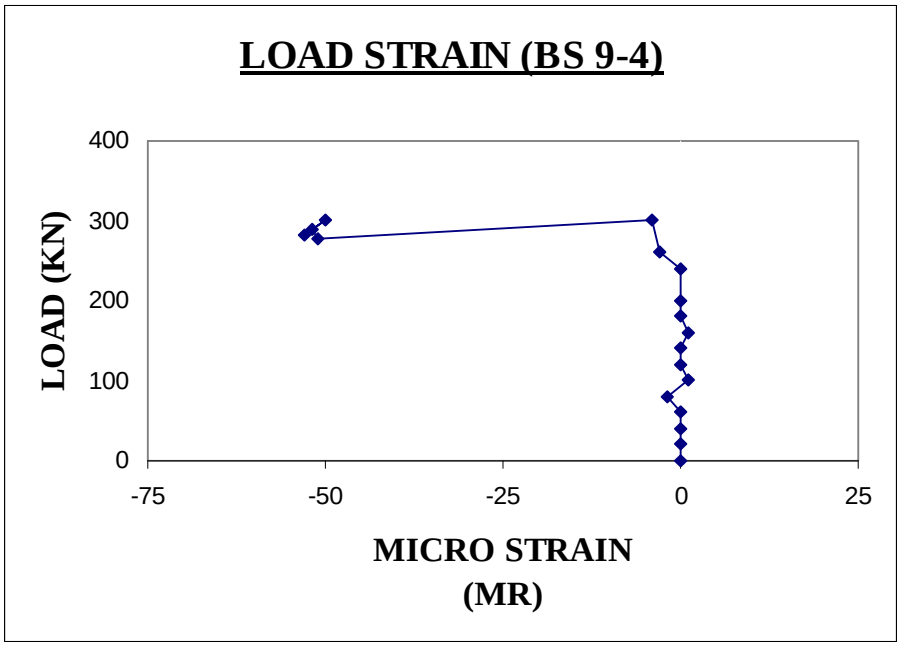

Fig 4.9 (a) Load strain behavior BS 9-4

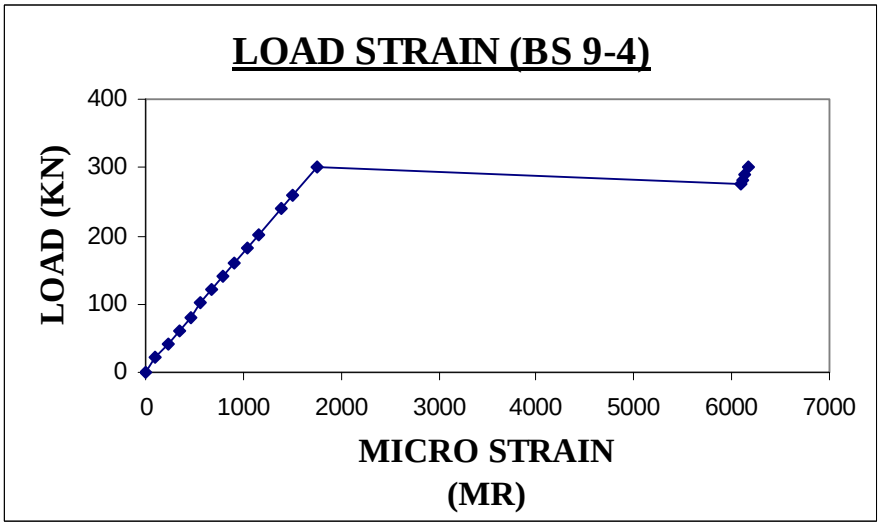

Fig 4.9 (b) Load strain behavior BS 9-4

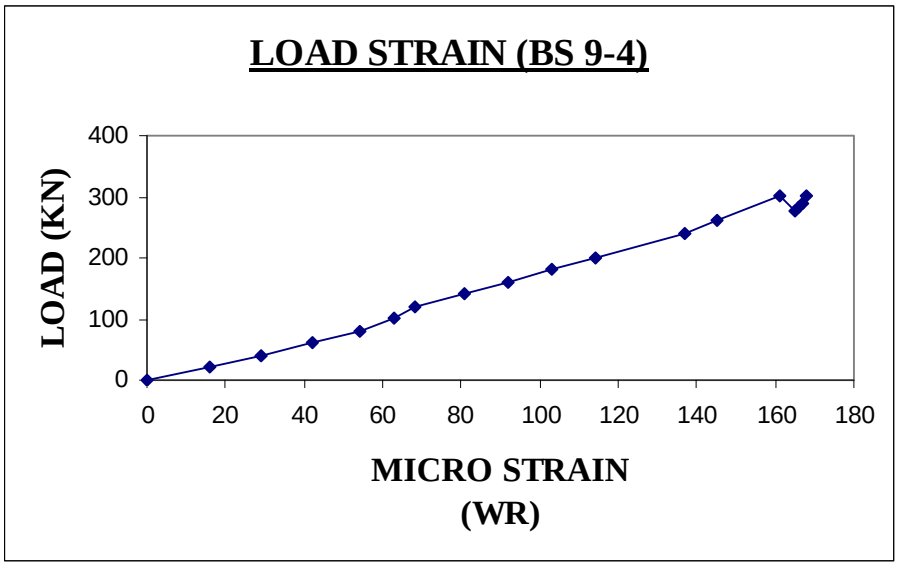

Fig 4.9 (c) Load strain behavior BS 9-4

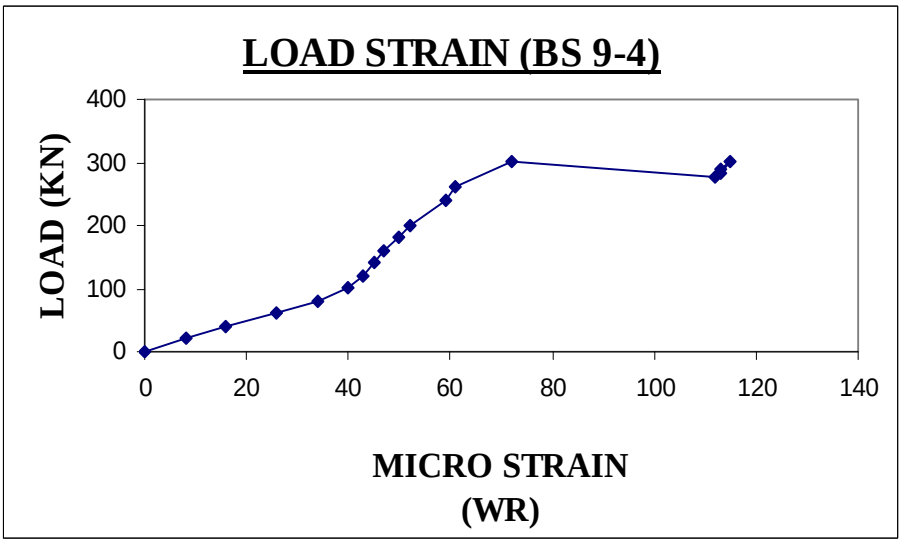

Fig 4.9 (d) Load strain behavior BS 9-4

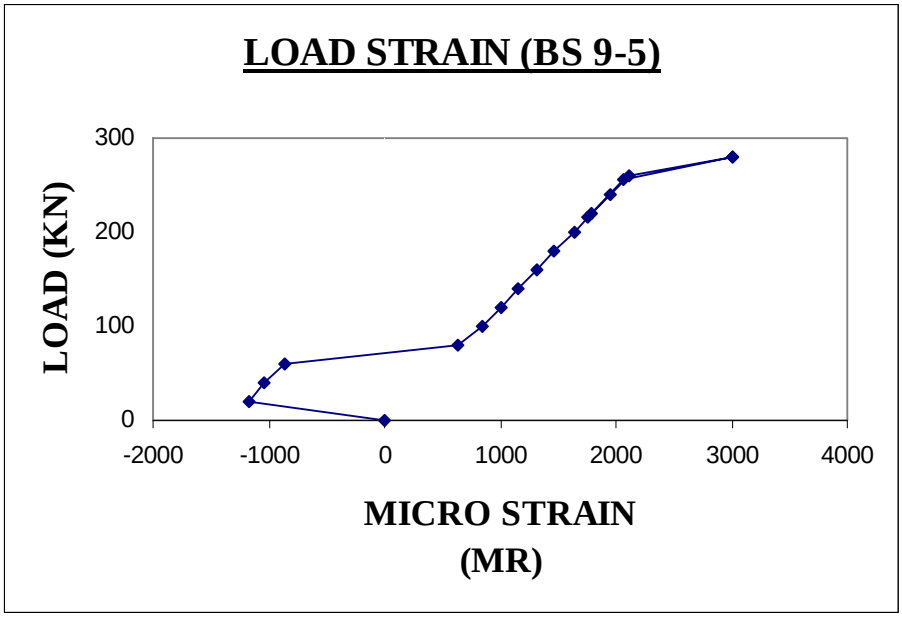

Fig 4.10 (a) Load strain behavior BS 9-5

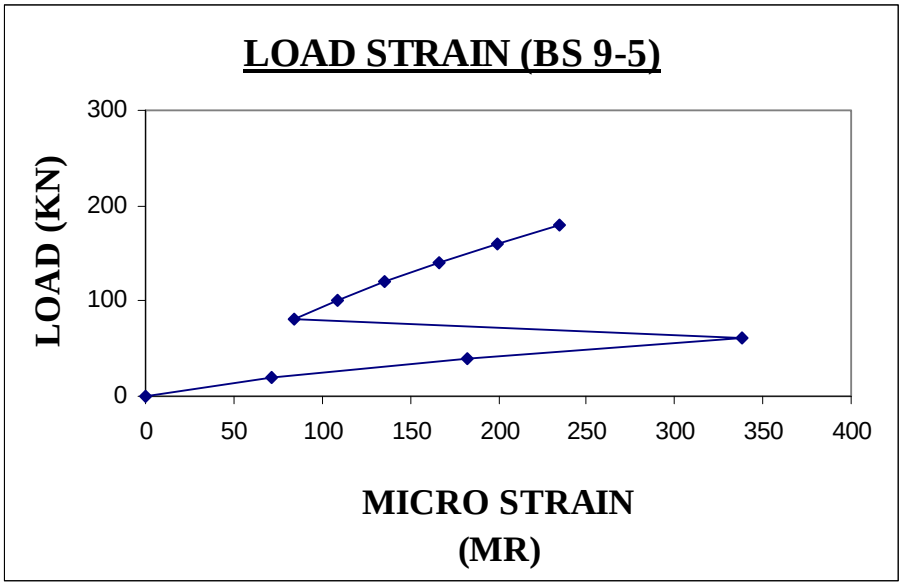

Fig 4.10 (b) Load strain behavior BS 9-5

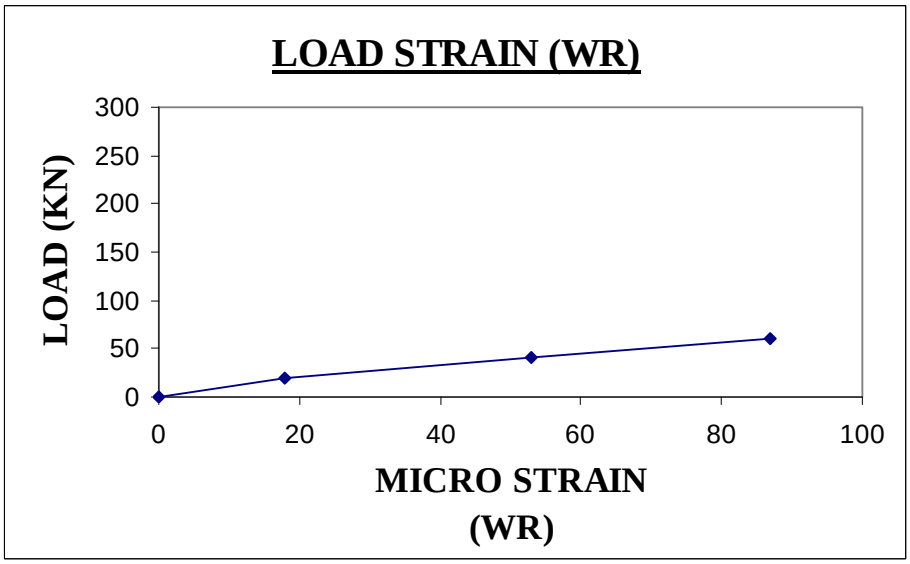

Fig 4.10 (c) Load strain behavior BS 9-5

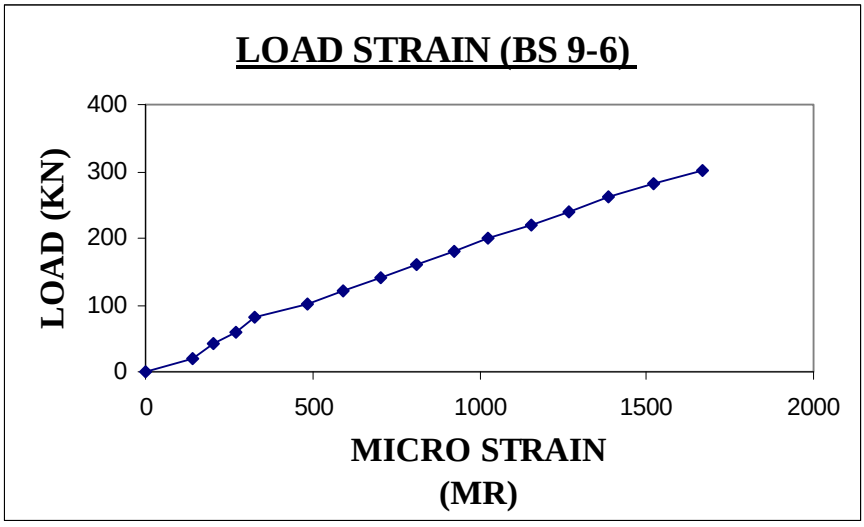

Fig 4.11 (a) Load strain behavior BS 9-6

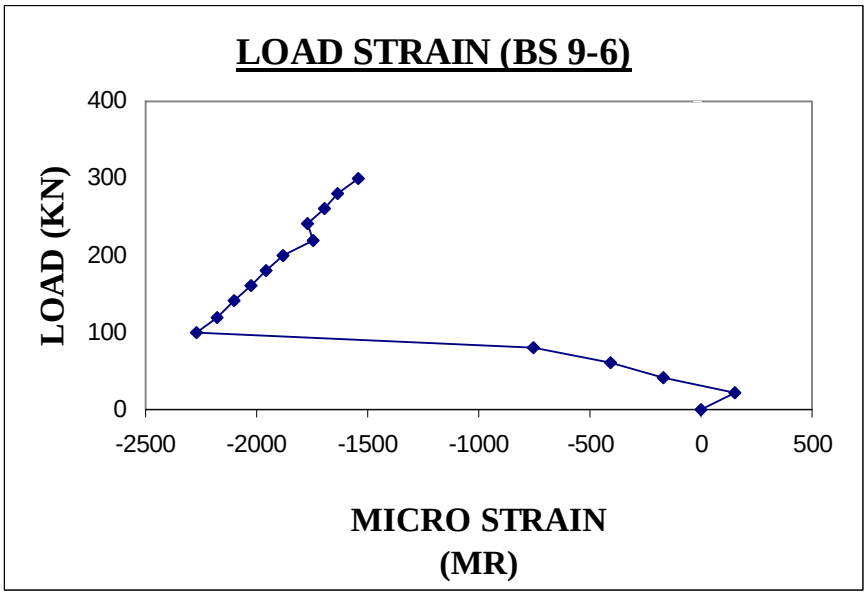

Fig 4.11 (b) Load strain behavior BS 9-6

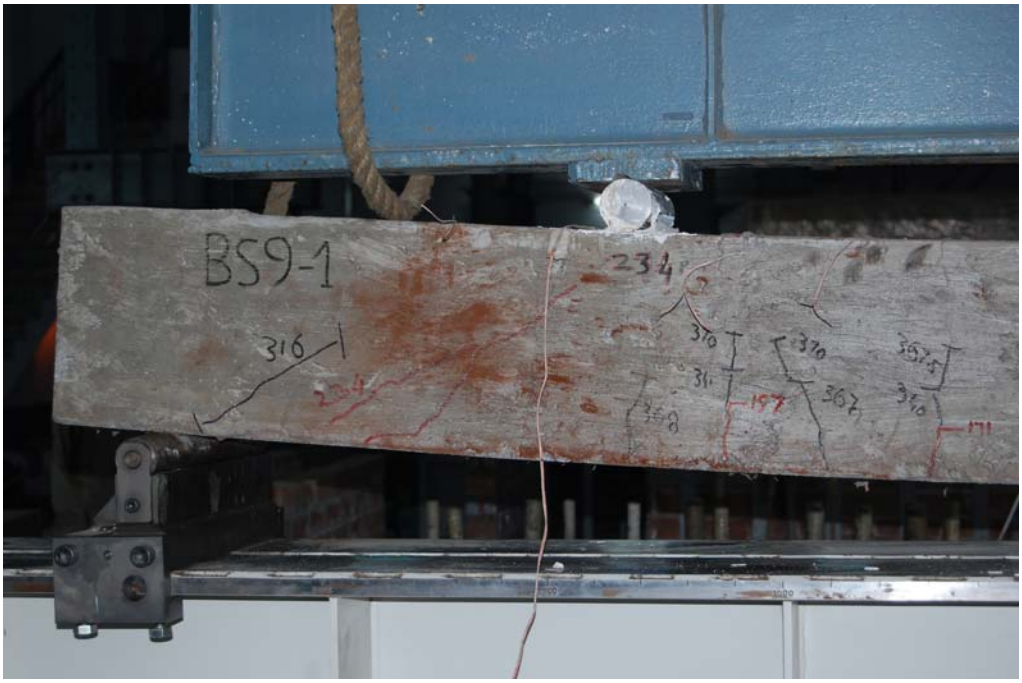

Fig 4.12 (a) Cracking pattern BS 9-1

Fig 4.12 (b) Cracking pattern BS 9-1

Fig 4.13 (a) Cracking pattern BS 9-2

Fig 4.13 (b) Cracking pattern BS 9-2

Fig 4.14 (a) Cracking pattern BS 9-3

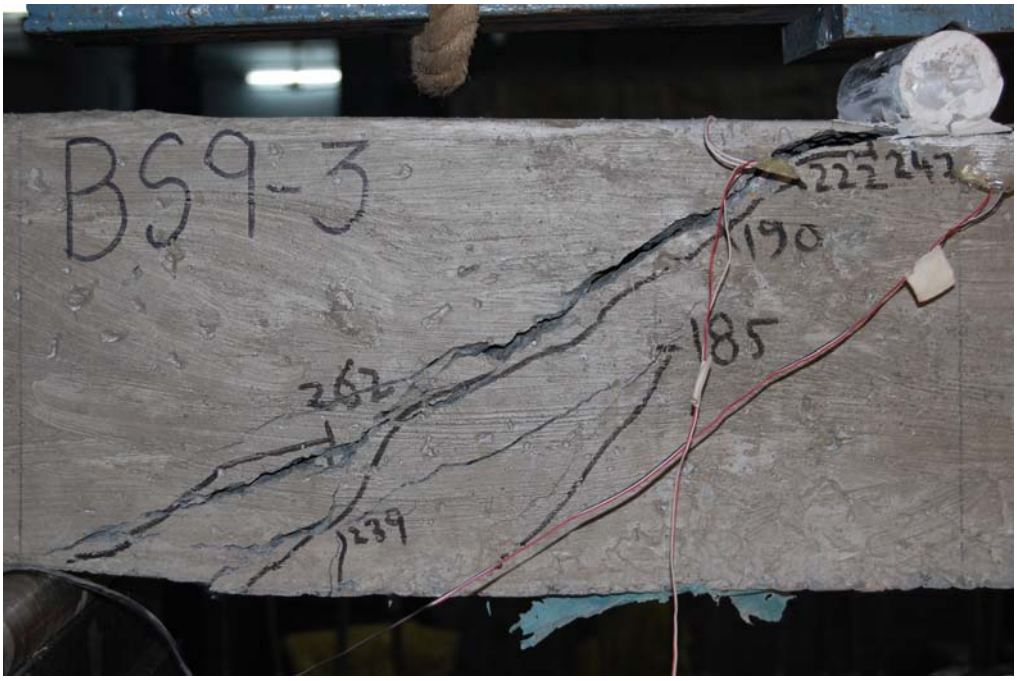

Fig 4.14 (b) Cracking pattern BS 9-3

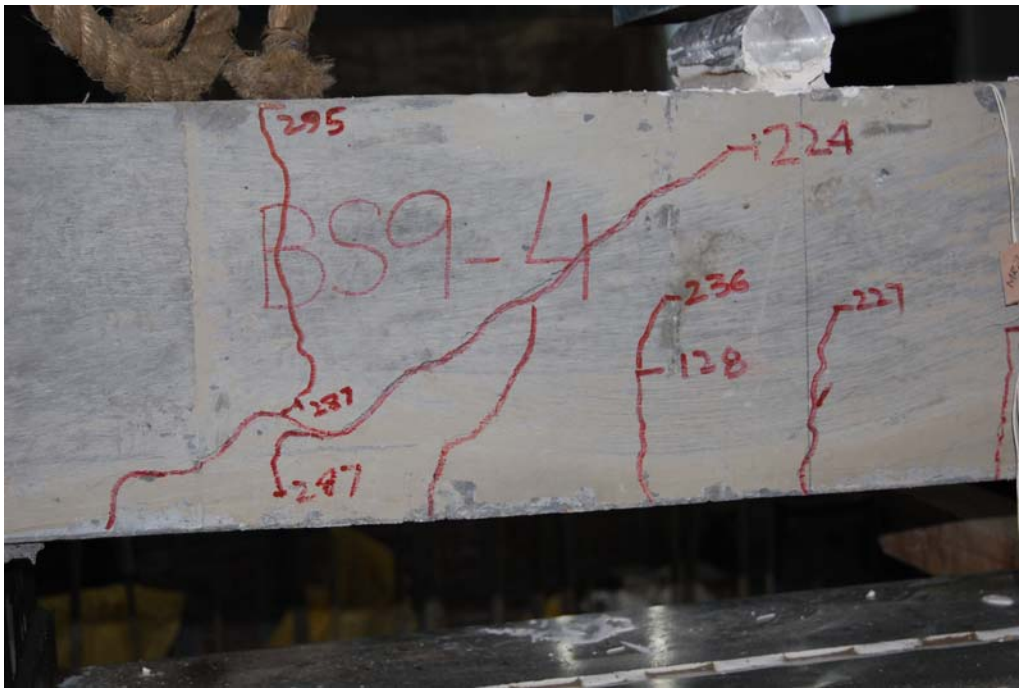

Fig 4.15 (a) Cracking pattern BS 9-4

Fig 4.15 (b) Cracking pattern BS 9-4

Fig 4.16 (a) Cracking pattern BS 9-5

Fig 4.16 (b) Cracking pattern BS 9-5

Fig 4.17 (a) Cracking pattern BS 9-6

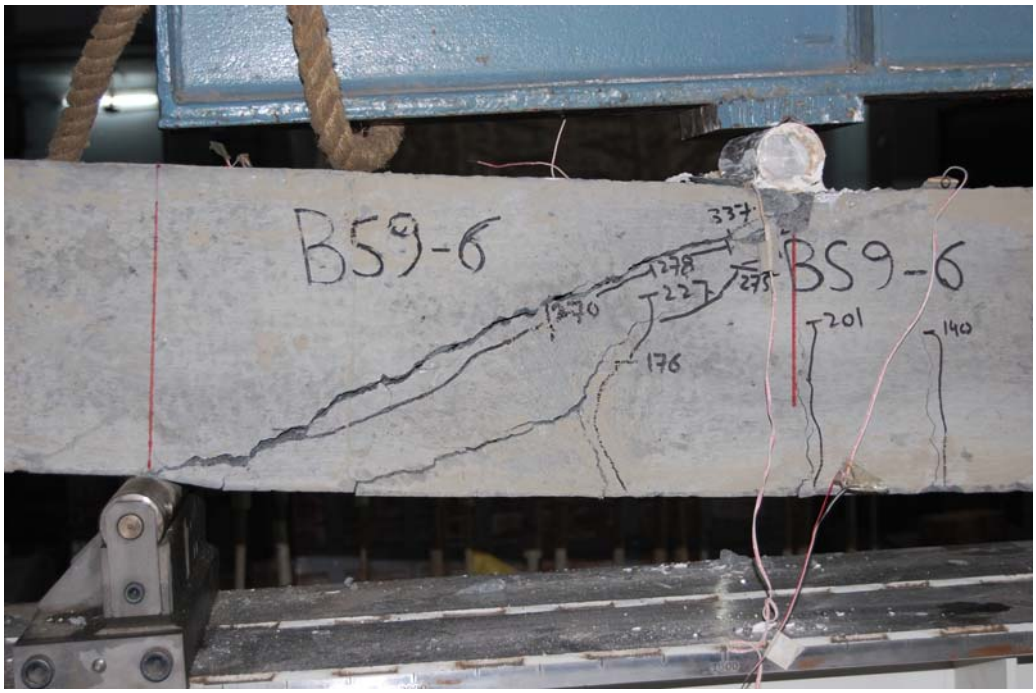

Fig 4.17 (b) Cracking pattern BS 9-6

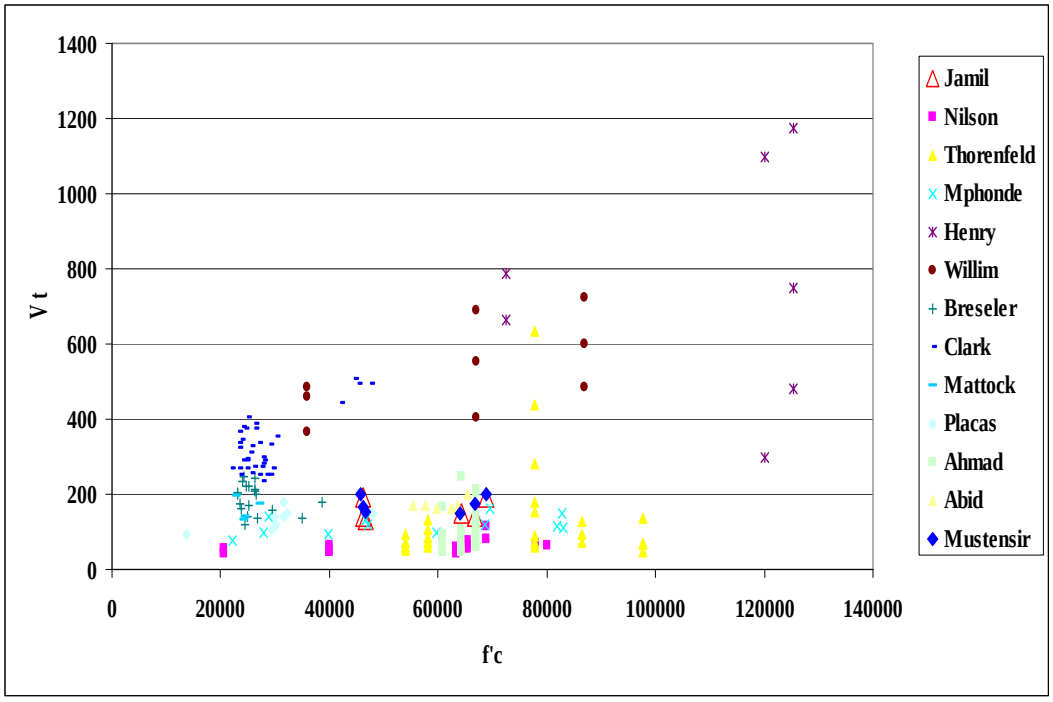

Fig 5.1 - V_t **as a function of** $f_c^{/}$

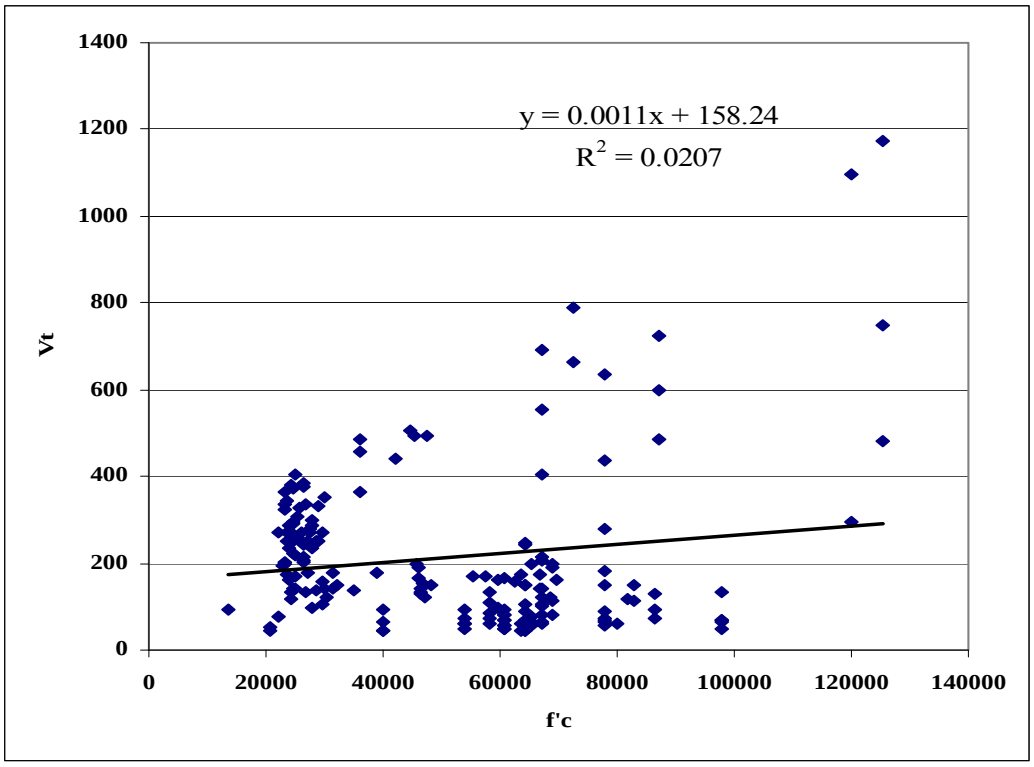

Fig 5.2 - V_t **as a function of** $f_c^{/}$

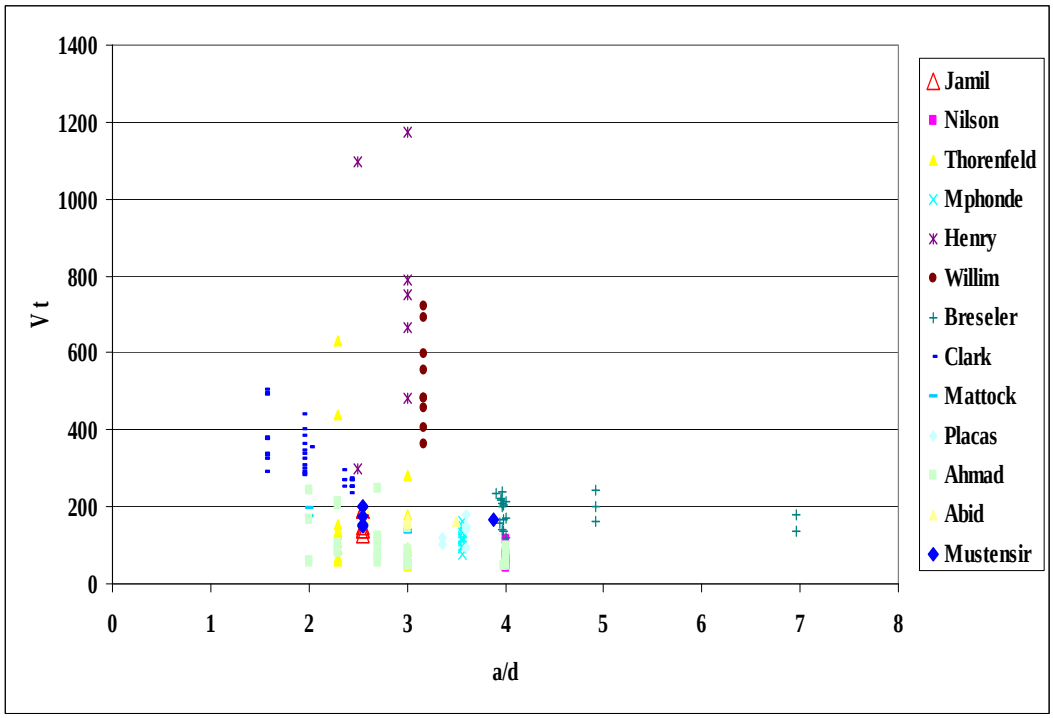

Fig 5.3 - V_t **as a function of** a/d

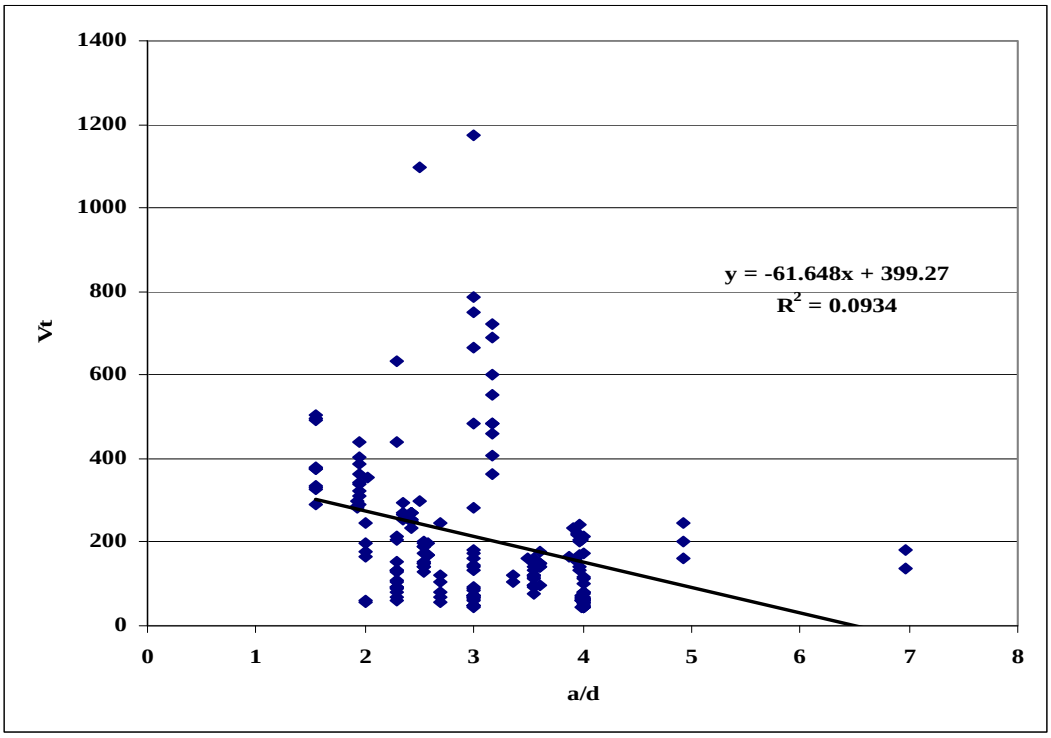

Fig 5.4 - V_t **as a function of** a/d

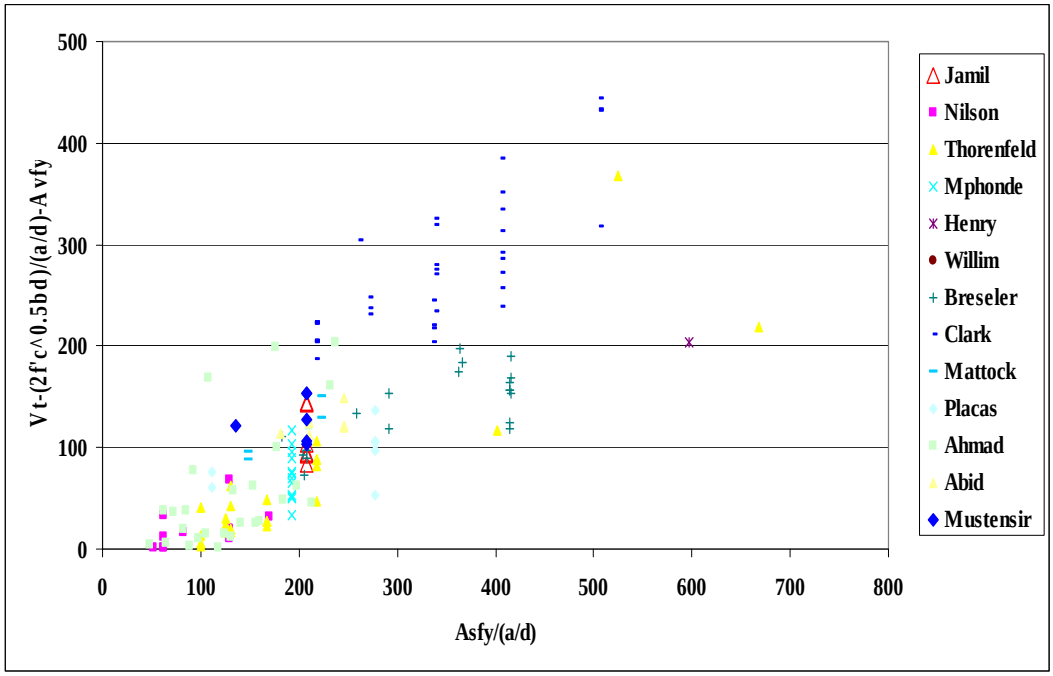

Fig 5.5 - $V_t - \frac{2\sqrt{f_c'}bd}{a/d} - A_V f_y$ **as a function of** $\frac{A_S f_y}{a/d}$

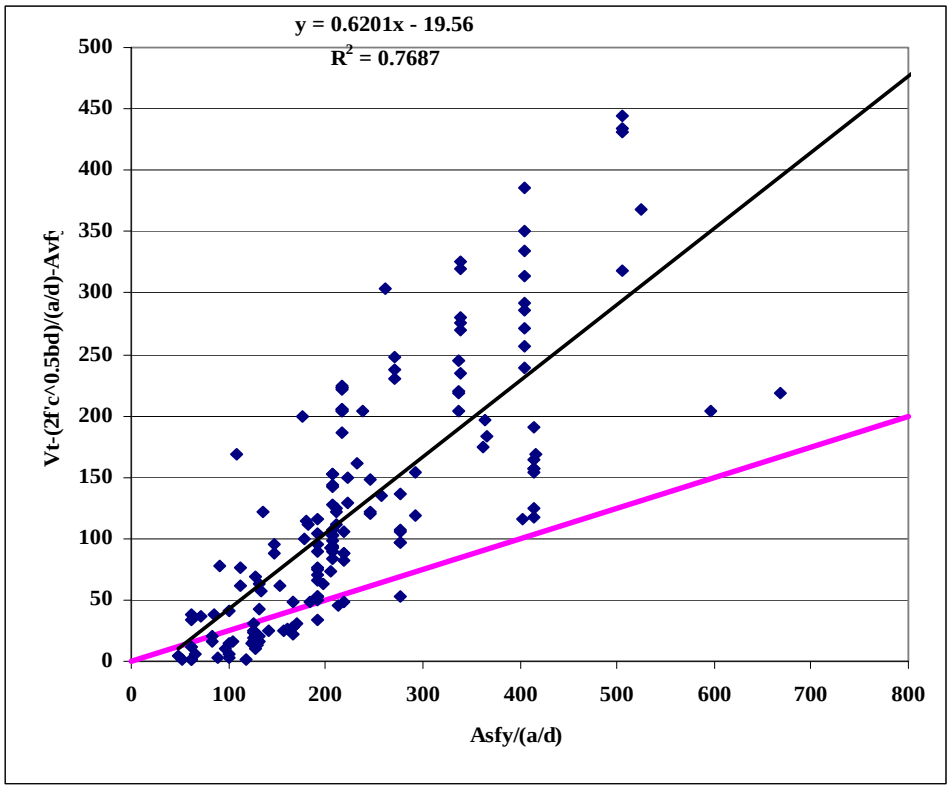

Fig 5.6 – Proposed Equation – $V_t - \frac{2\sqrt{f_c'}bd}{a/d} - A_V f_y$ **as a function of** $\frac{A_S f_y}{a/d}$

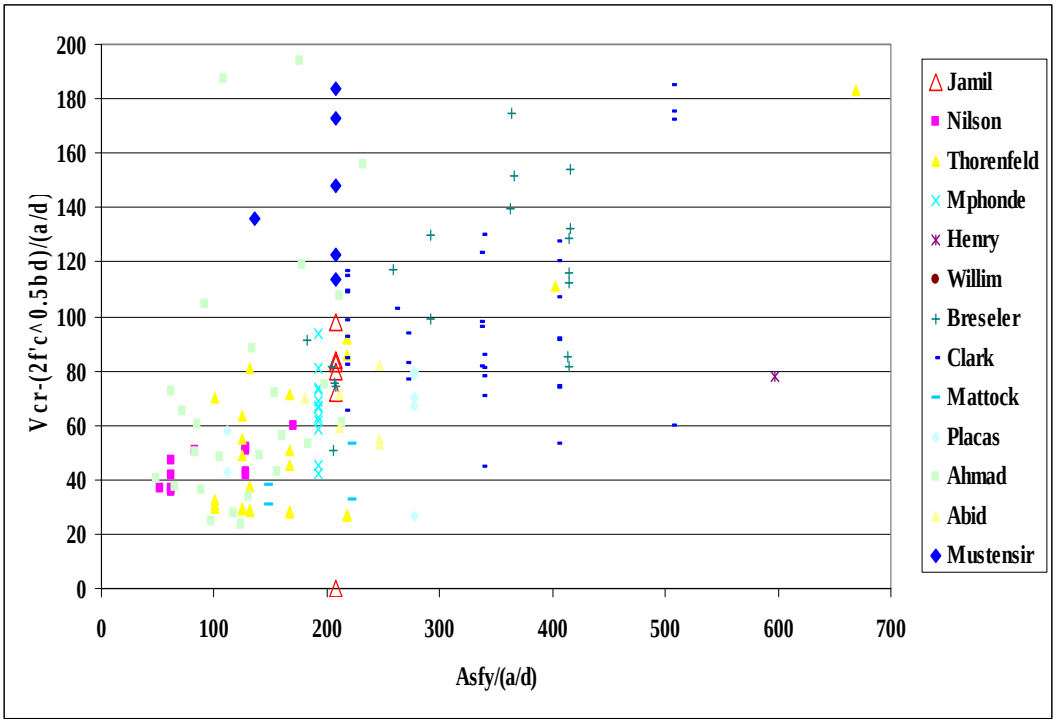

Fig 5.7 - $V_{cr} - \dfrac{2\sqrt{f_c'}bd}{a/d}$ **as a function of** $\dfrac{A_S f_y}{a/d}$

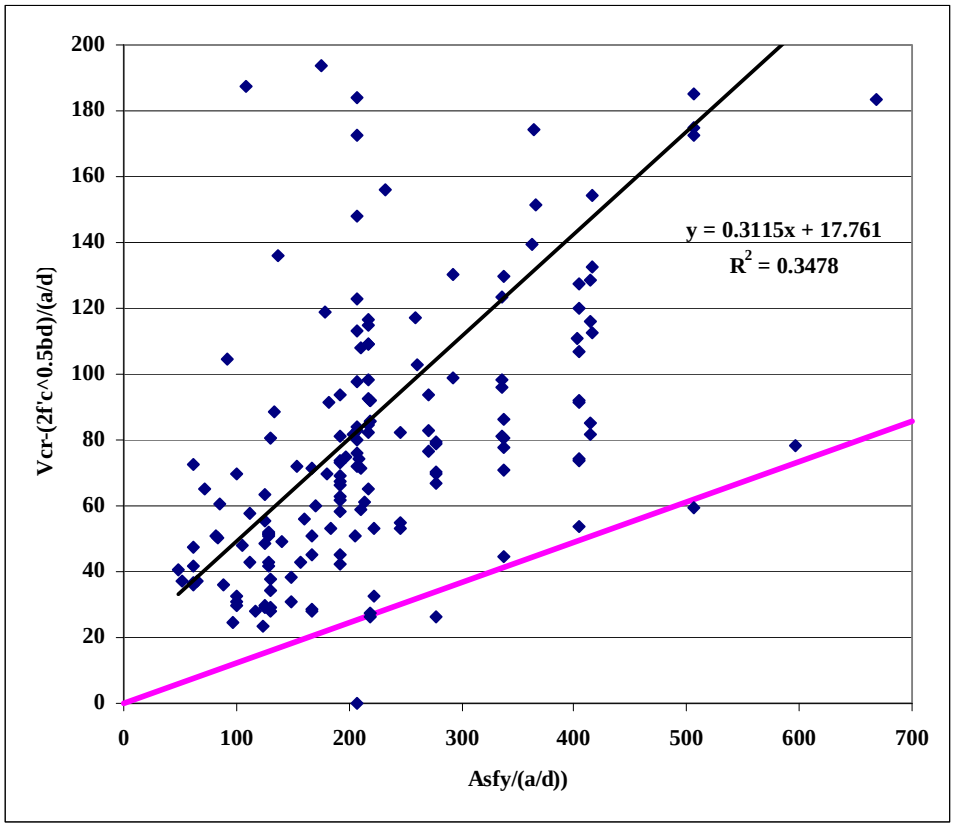

Fig 5.8 – Proposed Equation – $V_{cr} - \frac{2\sqrt{f_c'}bd}{a/d}$ **as a function of** $\frac{A_S f_y}{a/d}$

REFERENCES

- Building Code Requirements for Structural Concrete (AC1 318-05) and Commentary (ACI 318R-05), American Concrete Institute.
- Young-Soo Yoon, William D. Cook, and Denis Mitchell, "Minimum shear reinforcement in normal, medium, and high strength concrete beams", ACI structural journal, September-October 1996, pp 576-584.
- James G. Macgregor, "Reinforced Concrete Mechanics and Design", Prentice Hall, pp. 169-199.
- Arthur H. Nilson, "Design Implications of Current Research on High Strength Concrete", SP-87-7, pp.85-118.
- John J. Roller and Henry G. Russell, "Shear Strength of High-Strength concrete Beams with Web Reinforcement" ACI Structural Journal, March-April 1990, 87-S20, pp191-198.
- Edward G Nawy, PN Balaguru, "High-Strength Concrete", Pp 5-1 to 5-4.
- Mark K. Johnson and Julio A. Ramirez, "Minimum shear reinforcement in beams with higher strength concrete", ACI structural journal, July-August 1989, pp 376-382.
- Arthur H. Nilson / George winter, "Design of concrete structures". pp23-52.
- Design Implications of Current Research on High Strength Concrete by Arthur H. Nilson, ACI Special Publications, Sp-98, 1985.
- R. N. Swamy, "High Strength Concrete - Material Properties and structural Behavior", ACI Special Publications, SP-87, 1985.
- Andrew G. Mphonde and Gregory C. Frantz. "Shear Tests of High and Low Strength Concrete Beams with Stirrup", ACI Special Publications, SP-87, 1985.

- Mphonde, A.G and Frantz, G.C, "Shear Tests of High and Low strength concrete beams without stirrups", ACI Journal, Proceeding, V.81, No 4, July-August 1984, PP 35-357.
- N. Sakagvchi, K. Yammanobe, Y. Kitada, T. Kawachi, and S. Koda. "Shear Strength of High Strength Concrete members", ACI Special Publications, SP-121, 1990, PP 155-178.
- E. Thornfeldt and G. Drangsholt "Shear Capacity of Reinforced High Strength concrete Beams", ACI Special Publications, SP-121, 1990, PP 129-154.
- Woo Kim and Richard N. White "Inclination of Shear Cracking in Reinforced Concrete Beams with no Web Reinforcement", ACI structural Journal, Proceeding, May-June 1991, PP 301-308.
- "The Shear Strength of Reinforced Concrete members", By Joint ASCE-ACI Task Committee, Proceedings ASCE Journal, Vol 99, June 1973, PP 1019-1187.
- Joden Morrow and I. M. Viest, "Shear Strength of Reinforced Concrete Frame Members without Web Reinforcement", ACI Journal Vol - 53 March 1957, PP 871-888.
- High Strength Concrete By National Crushed Stone Association.